MARTIN MARIETTA ENERGY SYSTEMS LIBRARIES
3 4456 0070930 2

ORNL/TM-10020

ornl

OAK RIDGE NATIONAL LABORATORY

MARTIN MARIETTA

Strong Cyclotron Damping of Electron Cyclotron Waves in Nearly Parallel Stratified Plasmas

A. Fruchtman
K. Riedel
H. Weitzner
D. B. Batchelor

OAK RIDGE NATIONAL LABORATORY
CENTRAL RESEARCH LIBRARY
CIRCULATION SECTION
4500N ROOM 175
LIBRARY LOAN COPY
DO NOT TRANSFER TO ANOTHER PERSON
If you wish someone else to see this report, send in name with report and the library will arrange a loan.

OPERATED BY
MARTIN MARIETTA ENERGY SYSTEMS, INC.
FOR THE UNITED STATES
DEPARTMENT OF ENERGY

Printed in the United States of America. Available from
National Technical Information Service
U.S. Department of Commerce
5285 Port Royal Road, Springfield, Virginia 22161
NTIS price codes—Printed Copy: A04; Microfiche A01

This report was prepared as an account of work sponsored by an agency of the United States Government. Neither the United States Government nor any agency thereof, nor any of their employees, makes any warranty, express or implied, or assumes any legal liability or responsibility for the accuracy, completeness, or usefulness of any information, apparatus, product, or process disclosed, or represents that its use would not infringe privately owned rights. Reference herein to any specific commercial product, process, or service by trade name, trademark, manufacturer, or otherwise, does not necessarily constitute or imply its endorsement, recommendation, or favoring by the United States Government or any agency thereof. The views and opinions of authors expressed herein do not necessarily state or reflect those of the United States Government or any agency thereof.

ORNL/TM-10020
Dist. Category UC-20 g

Fusion Energy Division

STRONG CYCLOTRON DAMPING OF ELECTRON CYCLOTRON WAVES IN NEARLY PARALLEL STRATIFIED PLASMAS

A. Fruchtman*
K. Riedel+
H. Weitzner*
D. B. Batchelor

*Courant Institute of Mathematical Sciences, New York University, New York, N.Y. 10012
+Also of Courant Institute of Mathematical Sciences. Current address: Kurchatov Institute Moscow, USSR, American Embassy, PNC Box M, Helsinki, Finland 00140

Date Published: September 1986

Prepared by the
OAK RIDGE NATIONAL LABORATORY
Oak Ridge, Tennessee 37831
operated by
MARTIN MARIETTA ENERGY SYSTEMS, INC.
for the
U.S. DEPARTMENT OF ENERGY
under contract DE-AC05-84OR21400

MARTIN MARIETTA ENERGY SYSTEMS LIBRARIES
3 4456 0070930 2

CONTENTS

ABSTRACT. v

1. INTRODUCTION 1

2. WAVE EQUATION IN THE RESONANCE LAYER. 8

3. ANALYSIS OF THE INTEGRAL EQUATIONS. 20

4. NUMERICAL COMPUTATION OF STRONGLY DAMPED WAVES IN DENSE PLASMAS. 40

5. DISCUSSION. 48

REFERENCES. 51

ABSTRACT

Propagation of extraordinary mode waves in nearly parallel stratified plasmas (magnetic beach geometry) is investigated. Since the plasma is unable to shield out the right circular component of the electric field, these waves are very heavily damped. The resonance region is treated by a boundary layer expansion which reduces the problem to an integrodifferential system in one dimension. It is proved analytically that for moderate to high density, waves incident from the high field side are totally absorbed with no reflected wave. At very low density some transmission is possible, where the transmission coefficients are being given correctly by cold plasma theory. Numerical solution of the integrodifferential system shows that the power deposition profile can differ significantly from that predicted from a local WKB theory.

1. INTRODUCTION

In this paper we investigate the propagation and absorption of the extraordinary electron cyclotron mode in plasmas for which the gradient in magnetic field strength, $\underset{\sim}{\nabla}B$, is nearly parallel to the magnetic field lines $\underset{\sim}{B}$ (i.e., nearly parallel stratification). Such a configuration corresponds to wave damping at a magnetic beach as is found primarily in magnetic mirror geometry.[1,2] The physics involved is much different from the situation, extensively studied tokamaks, where $\underset{\sim}{\nabla}B$ and ∇n_e are nearly perpendicular to $\underset{\sim}{B}$ (perpendicular stratification).[3] Near cyclotron resonance, $\omega = \Omega_{ce}$, where ω = wave frequency and Ω_{ce} = electron cyclotron frequency, the electron response to the right circular component E_- of the wave electric field $\underset{\sim}{E}$ is very strong, that is, $J_- = O[E_-/(\omega - \Omega_{ce})]$. With perpendicular stratification, $k_{\|}$, the component on the wave parallel to $\underset{\sim}{B}$, is fixed whereas the perpendicular component $k_{\perp}$ varies weakly with Ω_{ce} near $\omega = \Omega_{ce}$. Since $\underset{\sim}{J}$ must be balanced by $\underset{\sim}{\nabla} \times \underset{\sim}{\nabla} \times \underset{\sim}{E} = O(k^2E)$ in Maxwell's equations, the plasma current shields out the right circular polarized component of $\underset{\sim}{E}$. In the cold plasma limit, $E_- \equiv 0$ at cyclotron resonance. As a result, in perpendicularly stratified plasmas cyclotron damping is a comparatively weak finite temperature effect due to Doppler or relativistic broadening of the cyclotron resonance. However, in parallel stratified plasmas $k_{\perp}$ is constant while $k_{\|}$ becomes very large near $\omega = \Omega_{ce}$. Thus in Maxwell's equations, terms $O(k_{\|}^2E_-)$ can balance terms $O[E_-/(\omega - \Omega_{ce})]$, and the shielding out of E_- does not occur. As a result, in parallel stratified plasma damping of cyclotron waves can be very strong, virtually independently of temperature.

The feature of strong damping appears at all levels of description. In the cold plasma model the wave fields are described by a wave equation of the form

$$\underset{\sim}{\nabla} \times \underset{\sim}{\nabla} \times \underset{\sim}{E} - \frac{\omega^2}{c^2}\underset{\sim}{E} = \frac{4\pi i\omega}{c}\, \underset{\sim}{\sigma} \cdot \underset{\sim}{E} \quad , \tag{1.1}$$

where $\underset{\sim}{\sigma}$ is the usual cold plasma conductivity tensor and we have assumed harmonic time dependence for $\underset{\sim}{E} \propto e^{-i\omega t}$. The dispersion relation obtained from Eq. (1.1) for a uniform plasma is of the form

$$A\, n_{\parallel}^4 + B(n_{\perp}^2)n_{\parallel}^2 + C(n_{\perp}^2) = 0 \quad , \tag{1.2}$$

where

$$A = \left(1 - \frac{\omega_{pe}^2}{\omega^2}\right)\left(1 - \frac{\Omega_{ce}^2}{\omega^2}\right)$$

and

$$\underset{\sim}{n} = c\underset{\sim}{k}/\omega \quad .$$

Thus one of the solutions of Eq. (1.2) for $n_{\parallel}$ (the extraordinary mode root) has a singularity that occurs at $\Omega_{ce} = \omega$, independent of $n_{\perp}$. For fixed $n_{\perp}$ there is an associated cutoff, $n_{\parallel} \to 0$, at lower magnetic field, $\Omega_{ce} < \omega$, given by

$$(\Omega_{ce})^2_{cutoff} = (\omega^2 - \omega_{pe}^2)\left(1 - \frac{\omega_{pe}^2/\omega^2}{1 - n_{\perp}^2}\right) \quad . \tag{1.3}$$

The extraordinary mode propagates on the high magnetic field side of the cyclotron resonance. As the wave approaches cyclotron resonance, $n_{\parallel}$ becomes infinite, the parallel phase velocity $\omega/k_{\parallel}$ vanishes, and the group velocity turns perpendicular to the magnetic field.

If one assumes the plasma to be purely parallel stratified along z [i.e., $\underset{\sim}{B}_0(\underset{\sim}{x}) = \hat{z}B_0(z)$, $n_e(\underset{\sim}{x}) = n_e(z)$], then Eq. (1.1) reduces to an ordinary differential equation that can be cast in the standard form of the Budden tunnelling problem[2]

$$\left[\frac{d^2}{d\xi^2} - K_0^2\left(1 + \frac{X_0}{\xi}\right)\right] V = 0 \quad , \tag{1.4}$$

where $\xi = \omega z/c$ and for small values of ω_{pe}^2/ω^2, $n_\perp^2$ the quantities k_0^2 and X_0 are given approximately by

$$K_0^2 = 1 - \frac{(2 - \omega_{pe}^2/\omega^2)n_\perp^2}{2(1 - \omega_{pe}^2/\omega^2)} \quad , \tag{1.5}$$

$$X_0^{-1} \simeq \frac{\omega^2}{\omega_{pe}^2}\,\frac{1}{B_0}\,\frac{dB_0}{d\xi}\left[1 - \frac{(1 - \omega_{pe}^2/\omega^2)n_\perp^2}{2(1 - \omega_{pe}^2/\omega^2) - n_\perp^2}\right] . \tag{1.6}$$

The solutions to Eq. (1.4) can be expressed in terms of Whittaker functions, and Stokes parameters giving reflection and transmission coefficients are easily derived. One finds that for the extraordinary mode incident on the resonance from the high field side, no reflection occurs and the fraction of power absorbed is

$$|A|^2 = 1 - e^{-\pi K_0 X_0} \ . \tag{1.7}$$

Even for quite modest plasma parameters (e.g., $n_e = 10^{12}/cm^3$, $\omega = 28$ GHz, $L \equiv \left[(dB/dz)/B\right]^{-1} = 20$ cm as found in EBT-S or TMX-U), the absorption coefficient differs from unity by less than 10^{-15}. Thus the cold plasma theory predicts complete wave absorption, and since there is no explicit dissipation mechanism included in the model, the absorption appears to occur entirely at the point $z = 0$ where the equation has a regular singular point. We obtain no information about the spatial absoprtion profile.

Additional insight can be gained by examining the <u>local</u> warm plasma dispersion for $k_\parallel$ at fixed $k_\perp$. For propagation along $\underset{\sim}{B}_0$ (i.e., $k_\perp = 0$) the Maxwellian plasma dispersion relation takes the simple form

$$k_\parallel^2 = 1 - \frac{\omega_{pe}^2}{\Omega_{ce}} \frac{1}{k_\parallel v_e} Z(\xi) \quad , \tag{1.8}$$

where $v_e = (2T_e/m_e)^{1/2}$, $\xi = (\omega - \Omega_{ce})/k_\parallel v_e$, and $Z(\xi)$ is the plasma dispersion function. Figure 1 shows solutions of this dispersion relation as a function of Ω_{ce}/ω for parameters $n_e = 10^{12}/cm^3$, $T_e = 300$ eV, $\omega = 2\pi \times 28$ GHz. Below the cutoff and well above the cyclotron resonance, $k_i = Im\{k_\parallel\} = 0$ and $k_r = Re\{k_\parallel\}$ agree with the cold plasma result. As cyclotron resonance is approached (i.e., $\omega - \Omega_{ce} \sim k_\parallel v_e$), some energetic particles become able to satisfy the Doppler shifted resonance condition $v_\parallel = (\omega - \Omega_{ce})/k_\parallel$ and k_i begins to increase. At the cyclotron resonance layer, $\omega = \Omega_{ce}$, the bulk of the distribution satisfies the Doppler resonance condition and damping is very strong, $k_i \sim k_r$.

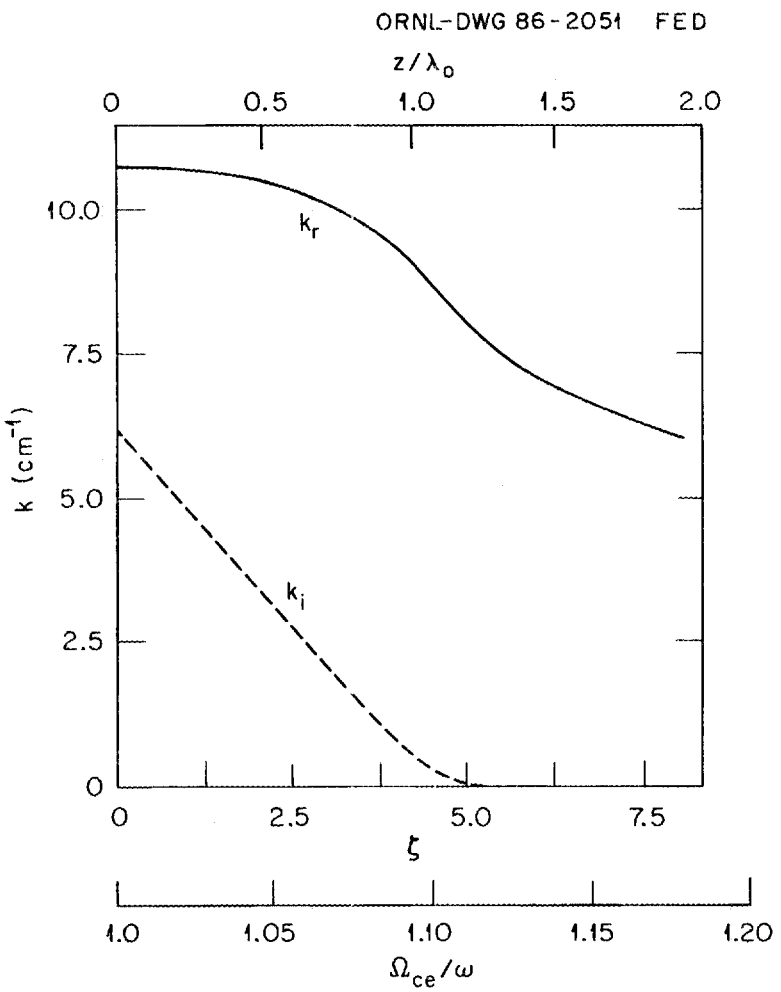

Fig. 1. Real and imaginary parts of k versus Ω_{ce}/ω and z/λ_o for $n_e = 10^{12}/cm^3$, $\omega/2\pi = 28$ GHz, $T_e = 300$ eV. Magnetic field scale length is L = 12 cm.

One can estimate the spatial structure of wave absorption by assuming geometrical optics and integrating $k_{\parallel}(z)$ as given by the local warm plasma dispersion relation

$$E(z) \simeq E_{\infty} \exp\left[i \int_{\infty}^{z} d\xi \, k_{\parallel}(\xi)\right] . \tag{1.9}$$

Using the plasma parameters listed above and assuming a linear magnetic field variation, $\Omega_{ce}(z) = \omega(1 + z/L)$, $L = 12$ cm, one finds that a wave propagating from $z = \infty$ is undamped until $z \lesssim 2.4$ cm (i.e., $\Omega_{ce}(z)/\omega \simeq 1.2$. Also, 95% of the incident power is absorbed by $z = 0.8$ cm (i.e., $\Omega_{ce}(z)/\omega \simeq 1.04$). Thus the wave is completely absorbed in 1.6 cm, a length comparable to one free space wavelength, $\lambda_0 \simeq 1.1$ cm. In this model the wave power at cyclotron resonance $z = 0$ is down from the incident power by 10^{-6}. Of course this WKB model would not show wave reflection even if it were actually present.

Although the local warm plasma WKB model gives an indication of the power dissipation profile and the spatial structure of $E(z)$, one can, in fact, have little confidence in its detailed correctness. In the first place, the rapid change in the plasma dispersive properties on the λ_0 space scale suggests the possible appearance of wave reflection and indicates the need for a full wave solution for the fields. In the second place, the plasma current in the local dispersion relation is calculated assuming that particles streaming along magnetic field lines see a wave field of the form $\underset{\sim}{E} \propto \exp\left[i(kv_{\parallel} - \omega)t\right]$ where $k_{\parallel}$ and $v_{\parallel}$ are constant. However, Fig. 1 shows that k varies significantly on the λ_0 scale and casts doubt on the very concept of a local wave number, a fundamentally geometrical optics concept. Also in reality $v_{\parallel}$ varies in parallel stratified plasmas due to the $\mu\underset{\sim}{\nabla}B$ force. In this paper we

present a self-consistent solution of the Vlasov-Maxwell system avoiding a WKB approximation for the wave fields and including the nonlocal character of the plasma current. A similar analysis has been carried out by Timofeev and Chalkor for the case that $\underset{\sim}{V}B$ makes a substantial angle with $\underset{\sim}{B}$. In this case E_- remains small, O(Ve/c), and the damping is comparatively weak. However, a nonlocal Greens function was found which is indentical to the one that appears in our analysis.

Our analysis confirms the result of cold plasma full wave theory that for high field incidence, no wave is reflected, and for moderate to high density, the incident power is completely absorbed. Furthermore, we are able to prove analytically that for a class of distribution functions satisfying certain assumptions of analyticity and behavior at infinity in $v_{\|}$, no wave is reflected and the transmitted wave (which exists only for very low density) is the same as given by the cold plasma model. Numerical solution of the integrodifferential equation shows that for some cases of interest the wave absorption profile differs significantly from that predicted by finite temperature WKB theory [Eq. (1.9)]. Even though the power is totally absorbed in a short distance, the shape of the absorption profile is of considerable practical importance. This is because the energy gain and velocity space diffusion experienced by a particle of given energy and pitch angle are roughly proportional to $|E_-|^2$ evaluated at the point along the field line Z_r at which the Doppler resonance condition is satisfied.

$$v_{\|}(Z_r) = \frac{\omega - \Omega_{ce}(Z_r)}{k_{\|}(Z_r)} \quad . \tag{1.10}$$

Thus, for example, large $v_{\parallel}$ particles that are resonant at large Z_r are strongly scattered by the full, undamped wave field, whereas small $v_{\parallel}$ particles that are resonant near $\Omega_{ce}(Z_r) = \omega$ experience only the damped wave fields and are not heated. Correct calculation of $E_-(z)$ is essential to correct calculation of quasi-linear diffusion.

2. WAVE EQUATION IN THE RESONANCE LAYER

We start from the Vlasov equation linearized about a zeroth order distribution function which is isotropic in velocity space

$$i\omega f + \underset{\sim}{v} \cdot \underset{\sim}{\nabla} f + \left(e/mc\right)\underset{\sim}{v} \times \underset{\sim}{B}o \cdot \underset{\sim}{\nabla}_{\underset{\sim}{v}} f = -\left(e/m\right)\underset{\sim}{E} \cdot \underset{\sim}{v} \frac{\partial F}{\partial v^2/2} \quad , \tag{2.1}$$

and from Maxwell's equations written as

$$\left(c^2/\omega^2\right)\underset{\sim}{\nabla} \times \left(\underset{\sim}{\nabla} \times \underset{\sim}{E}\right) - \underset{\sim}{E} = -\left(4\pi e i/\omega\right) \int f \underset{\sim}{v} d \ , \tag{2.2}$$

where we have assumed time harmonic dependence of all linearized variables of the form $\exp(i\omega t)$, and where the causality condition requires that the solution be extendible into the domain $\mathrm{Re}(i\omega) > 0$ or $\mathrm{Im}\omega < 0$ and that the solution tend to zero as $\mathrm{Im}\omega \to -\infty$. For simplicity we assume an equilibrium magnetic field with only $\hat{x}$ and $\hat{z}$ components

$$\underset{\sim}{B}_0 = B_0\left(x, z\right)\left[\hat{x} \sin \alpha\left(x, z\right) + \hat{z} \cos \alpha\left(x, z\right)\right] = B_0 \hat{b}_0\left(x, z\right) \ . \tag{2.3}$$

We assume that all equilibrium quantities vary slowly with respect to the free space wavelength c/ω. Thus, geometrical optics applies except

in the immediate vicinity of the fundamental cyclotron resonance where wave absorption is strong.

The assumption that all equilibrium quantities vary slowly in space relative to the free space wavelength may be given explicitly by the requirement that any equilibrium function of space, say c(x, y, z) is of the form

$$c(x, y, z) = C\left(\delta x\omega/c,\ \delta y\omega/c,\ \delta z\omega/c\right) , \tag{2.4}$$

where δ is the usual geometrical optics small expansion parameter. We specify δ quite specifically shortly. We must assume that the first few derivatives of B(x, y, z) with respect to x, y, and z are all of order one in δ and in any other small parameters we introduce. Our analysis depends on the presence of one other small parameter, namely the ratio of the mean electron thermal speed to the speed of light

$$\varepsilon = v_{th}/c . \tag{2.5}$$

Our earlier study of geometrical optics in plasma at electron cyclotron frequencies[4,5] required that ε be small as well as δ. Here we shall be forced to make specific assumptions relating ε and δ in order to find nontrivial resonance layer approximations to the system (2.1) and (2.2). We consider two distinct cases. In the first we assume that the ratio of the electron plasma frequency, ω_{pe}, to the electron cyclotron frequency, Ω_{ce}, is zero order in both ε and δ. In the second low density case, which includes Budden tunnelling, we assume ω_{pe}/Ω_{ce} small. The requirement of nontrivial resonance layer equations finally imposes specific scaling relationships between ε, δ, and ω_{pe}/Ω_{ce}. Beyond the

range of these relationships our treatment most likely fails. Before we start the resonance layer expansion, it is convenient to recast the Vlasov equation in a different form in dimensionless variables. Our choice of space coordinates, nondimensional relative to the free space wavelength – as opposed to charateristic equilibrium gradient length – implies that we have already partially completed the stretching of variables typical of an inner expansion in a boundary layer theory. Further, in our coordinates we generally expect geometrical optics expansions of the form $\underset{\sim}{E} \sim \underset{\sim}{E}_0(\delta\tilde{x}, \delta\tilde{y}, \delta\tilde{z})\exp[i\Phi(\tilde{x}, \tilde{y}, \tilde{z})]$, where the space variables are $\tilde{x}$, $\tilde{y}$, and $\tilde{z}$ measured in units of the inverse free space wave number. Specifically, we introduce nondimensional space and velocity space variables by the definitions

$$\underset{\sim}{x} = \left(c/\omega\right)\underset{\sim}{\tilde{x}} \quad , \tag{2.6}$$

$$\underset{\sim}{v} = v_{th}\underset{\sim}{u} \quad , \tag{2.7}$$

and modified distribution functions $g(\underset{\sim}{\tilde{x}}, \underset{\sim}{u})$, $G(u^2/2)$

$$F\left(\underset{\sim}{v}\right)d\underset{\sim}{v} = n_0 G\left(\underset{\sim}{u}\right)d\underset{\sim}{u} \ , \tag{2.8}$$

where

$$\int G\left(\underset{\sim}{u}\right)d\underset{\sim}{u} = 1 \quad , \tag{2.9}$$

$$4\pi e\ F(\underset{\sim}{v})d\underset{\sim}{v} = v_{th}g(\underset{\sim}{u})d\underset{\sim}{u} \quad , \tag{2.10}$$

and n_0 is the local electron number density. The original Vlasov-Maxwell system (2.1) and (2.2) becomes

$$i\omega g + \varepsilon\omega(\underset{\sim}{u} \cdot \tilde{\underset{\sim}{\nabla}})g + \left[e/(mc)\right]\underset{\sim}{u} \times \underset{\sim}{B}_0 \cdot \underset{\sim}{\nabla}_u g = -\omega_{pe}^2 \underset{\sim}{E} \cdot \underset{\sim}{u} \frac{\partial G}{\partial u^2/2} \quad , \tag{2.11}$$

and

$$\tilde{\underset{\sim}{\nabla}} \times (\tilde{\underset{\sim}{\nabla}} \times \underset{\sim}{E}) - \underset{\sim}{E} = \int d\underset{\sim}{u}\; g(\underset{\sim}{u}, \tilde{\underset{\sim}{x}})(d\underset{\sim}{u})/(i\omega) \equiv \underset{\sim}{J}/(i\omega) \quad . \tag{2.12}$$

We have effectively assumed in (2.8) that the equilibrium distribution function is spatially independent. This assumption is clearly not essential but neither is it restrictive since our analysis is finally localized to the neighborhood of a point on the resonance surface. We take $G(\underset{\sim}{u})$ to be the distribution function at that point.

Proceeding similarly to the analysis of Ref. 6, we introduce components of $\underset{\sim}{u}$ parallel to and perpendicular to $\hat{b}_0$ by the definitions

$$\underset{\sim}{u} = u_{\parallel}\hat{b}_0 + u_{\perp}\cos\phi\left(\hat{y} \times \hat{b}_0\right) + u_{\perp}(\sin\phi)\hat{y} \ , \tag{2.13}$$

where ϕ is the angle of the gyrophase and we expand g in a Fourier series in ϕ

$$g = \sum_{m=-\infty}^{\infty} g_m\left(u_{\perp}, u_{\parallel}, \tilde{\underset{\sim}{x}}\right)e^{im\phi} \ . \tag{2.14}$$

When we change the independent variables in the Vlasov equation from $(\tilde{\underset{\sim}{x}}, \underset{\sim}{u})$ to $(\tilde{\underset{\sim}{x}}, u_{\parallel}, u_{\perp}, \phi)$ and when we employ the expansion (2.14), we find that (2.11) becomes the infinite set of coupled equations

$$i\left(\omega + n\Omega_{ce}\right)g_n + \varepsilon\omega\left[u_{\parallel}\left(\hat{\underset{\sim}{b}}_0 \cdot \tilde{\underset{\sim}{\nabla}}\right) + \frac{1}{2}u_{\perp}\left(\hat{y} \times \hat{b}_0 \cdot \tilde{\underset{\sim}{\nabla}}\alpha\right)\left(u_{\perp}\frac{\partial}{\partial u_{\parallel}} - u_{\parallel}\frac{\partial}{\partial u_{\perp}}\right)\right]g_n$$

$$+ \varepsilon\omega\left(0_n^{+2}g_{n+2} + 0_n^{+1}g_{n+1} + 0_n^{-1}g_{n-1} + 0_n^{-2}g_{n-2}\right)$$

$$= -\omega_{pe}^2 \frac{\partial G}{\partial u^2/2}\left[E_{\parallel}u_{\parallel}\delta_n^0 + \frac{1}{2}u_{\perp}\left(E_+\delta_n^{+1} + E_-\delta_n^{-1}\right)\right] , \tag{2.15}$$

where

$$\Omega_{ce} = |e|B_0/mc > 0 \quad , \tag{2.16}$$

$$E_{\parallel} = \hat{b}_0 \cdot \underset{\sim}{E} \quad , \tag{2.17}$$

$$E_{\pm} = \mp iE_y + \hat{y} \times \hat{b}_0 \cdot \underset{\sim}{E} \quad , \tag{2.18}$$

and 0_n^m, $m \neq 0$ are first-order spatial differential operators given in Ref. 7 whose specific form we do not need here. We note, however, that they contain only spatial gradients of perturbed quantities only in the directions perpendicular to $\hat{b}_0$. In direct analog with (2.17) and (2.18), we may define the $\parallel$ and $\pm$ components of any vector, in particular the current, and

$$J_{\parallel} = \int u_{\parallel}u_{\perp}g_0 du_{\parallel}du_{\perp}d\phi \quad , \tag{2.19}$$

$$J_{\pm} = \int u_{\perp}^2 g_{\pm 1}du_{\parallel}du_{\perp}d\phi \ . \tag{2.20}$$

Examining the Vlasov equation in the form (2.15), we see that for ε small only the $n = -1$ component is significantly affected by the

fundamental cyclotron resonance. To leading order in ε we find, just as the nonresonant case,

$$g_0 = i(\omega_{pe}^2/\omega)u_{\parallel}E_{\parallel}\frac{\partial G}{\partial u^2/2} \quad , \tag{2.21}$$

and

$$g_{+1} = -\frac{1}{2}i\left[\omega_{pe}^2/(\omega + \Omega_{ce})\right]u_{\perp}E_{\perp}\frac{\partial G}{\partial u^2/2} \quad , \tag{2.22}$$

from which we obtain [see (2.19) and (2.20)]

$$J_{\parallel} = -i\left(\omega_{pe}^2/\omega\right)E_{\pm} \quad , \tag{2.23}$$

and

$$J_{+} = -i\left[\omega_{pe}^2/\left(\omega + \Omega_{ce}\right)\right]E_{\perp} \quad . \tag{2.24}$$

One can verify a postiori that contributions to g_0 and g_{+1} from g_{-1} are smaller than the terms retained in (2.21) and (2.22). Clearly the forms (2.23) and (2.24) are exactly the same as given by the cold plasma conductivity tensor for the nonresonant components.

To proceed, we perform a boundary layer analysis on Eq. (2.15) with $n = -1$ in the fundamental cyclotron resonance region. We mix the methods of the geometrical optics approximation in two space coordinates perpendicular to $\underset{\sim}{\nabla}B$ together with a boundary layer stretching in the space coordinate along $\underset{\sim}{\nabla}B$. A central element of this formal analysis is the assumption that the medium is approximately parallel stratified on the resonance surface. That is, we assume that $\hat{b}_0$ and $\tilde{\underset{\sim}{\nabla}}B_0$ are nearly

parallel on the resonance surface. Further, since $\hat{b}_0$ and $\tilde{\underset{\sim}{\nabla}}B_0$ change slowly in space, we may take $\hat{b}_0$ and $\hat{\nabla}B_0$ as approximately parallel for some number of free space wavelengths in the neighborhood of the resonance surface. We now start the introduction of our resonance layer coordinates. For any given point in space $(\tilde{x}, \tilde{y}, \tilde{z})$ we construct a straight line normal to the resonance surface from that point to the resonance surface. Our two transverse coordinates are the quantities $\zeta(\tilde{x}, \tilde{y}, \tilde{z})$ and $\eta(\tilde{x}, \tilde{y}, \tilde{z})$ which parameterize the point on the surface at the foot of the normal. We might take as the third coordinate $(\Omega_{ce} - \omega)/\omega$, which clearly measures the distance along the normal, but in view of (2.4) we see that $(\Omega_{ce} - \omega)/\omega$ is of order δ in the entire resonance layer. Thus, we introduce the stretched coordinate ξ by the definition

$$\xi\omega\delta = \Omega_{ce} - \omega \quad . \tag{2.25}$$

Hence, we may parameterize space by the coordinates ξ, η, and ζ. Provided the fundamental resonance surface be smooth, the equilibrium quantities are functions of $\delta\xi$, $\delta\eta$, and $\delta\zeta$ only. In this coordinate system $\xi = 0$ is the resonance surface and $|\xi| \sim 1$ constitutes the entire resonance layer region.

The Vlasov-Maxwell system (2.15) and (2.16) exhibits singular behavior at fundamental resonance only in the coordinate ξ, and it is well-behaved in the coordinates ζ and η in which it is slowly varying. Thus, we can employ a geometrical optics approximation in these coordinates and $\partial/\partial\xi \to ik_\xi$, $\partial/\partial\eta \to ik_\eta$, and in view of the approximate parallel stratification, a perpendicular wave number vector $\underset{\sim}{k}_\perp$ is well-defined. Hence $\underset{\sim}{k}_\perp$, which is O(1), varies slowly in space and is determined by a limiting procedure of geometrical optics as one

approaches resonance. When $\underset{\sim}{\nabla}_\perp$ is replaced by $i\underset{\sim}{k}_\perp$, we have reduced our system to one space coordinate ξ only. If we differentiate (2.25), we find

$$(\hat{B}_0 \cdot \nabla)\xi\omega\delta = (\hat{b}_0 \cdot \tilde{\underset{\sim}{\nabla}}\Omega_{ce}) ,$$

and we finally define δ precisely by

$$\delta = \hat{b}_0 \cdot \tilde{\underset{\sim}{\nabla}}\Omega_{ce}/\omega > 0 , \tag{2.26}$$

where $\delta(\zeta, \eta)$ is evaluated at a particular point on the resonance surface. We may now rewrite (2.15) with $n = -1$ in the form

$$-i\delta\xi g_{-1} + \varepsilon u_\parallel \frac{\partial g_{-1}}{\partial \xi} + \frac{1}{2}\left(\omega_{pe}^2/\omega\right)u_\perp E_- \frac{\partial G}{\partial u^2/2}$$

$$= \varepsilon\left[\frac{u_\perp}{2}\left(\hat{y} \times \hat{b}_0\tilde{\underset{\sim}{\nabla}}\alpha\right)\left(u_\perp\frac{\partial}{\partial u_\parallel} - u_\parallel\frac{\partial}{\partial u_\perp}\right) - iu_\parallel k_\eta\left(\hat{b}_0 \cdot \tilde{\underset{\sim}{\nabla}}\eta\right) - iu_\parallel k_\xi(\hat{b}_0 \cdot \tilde{\underset{\sim}{\nabla}}\xi)\right]g_{-1}$$

$$+ \varepsilon\left(0_{-1}^{2}g_1 + 0_{-1}^{1}g_0 + 0_{-1}^{-1}g_{-2} + 0_{-1}^{-2}g_{-3}\right) . \tag{2.27}$$

To leading order we may drop all terms on the right-hand side, as these terms may be shown, a postiori, to be smaller than the terms retained. Thus, g_{-1} is determined as the solution of the comparatively simple equation

$$i\delta\xi g_{-1} + \varepsilon u_\parallel\frac{\partial g_{-1}}{\partial \xi} = -\frac{1}{2}u_\perp\left(\omega_{pe}^2/\omega\right)\frac{\partial G}{\partial u^2/2} E_- . \tag{2.28}$$

For ξ large the first term on the left-hand side of (2.28) dominates, and we are back to the cold plasma conductivity tensor. We shall consider only the cases $\delta/\varepsilon \sim 1$ and $\delta/\varepsilon > 1$. For δ/ε small our analysis most likely does not apply.

It is convenient to make a last change of variables to obtain a compact representation of the solution of (2.28). We set

$$\xi' = (\varepsilon/\delta)^{1/2}\ \xi \quad , \tag{2.29}$$

and we may write the unique causal solution of (2.28) as

$$(\varepsilon\delta)^{1/2}\ g_{-1} = -\frac{1}{2}\left(\omega_{pe}^2/\omega\right)\frac{\partial G}{\partial u_\perp}\int_{-\infty\mathrm{sgn}(u_\parallel)}^{\zeta'} d\xi/u_\parallel)E_-(\xi)\exp\left[i\left(\xi'^2 - \xi^2\right)/u_\parallel\right] ,$$

so that

$$J_- = \frac{\omega_{pe}^2}{\omega}\frac{1}{(\varepsilon\delta)^{1/2}}\int u_\perp du_\perp du_\parallel d\phi\frac{G(u)}{u_\parallel}\int_{-\infty\mathrm{sgn}(u_\parallel)}^{\xi'} d\xi\ E_-(\xi)\exp\left[i\left(\xi'^2 - \xi^2\right)/u_\parallel\right] . \tag{2.30}$$

We see from (2.23), (2.24), and (2.30) that near resonance J_+ is of order $E_+\omega_{pe}^2/\omega$, $J_\parallel$ is of order $E_\parallel\omega_{pe}^2/\omega$, while J_- is of order $E_-\left[(\omega_{pe}^2/\omega)/\sqrt{\varepsilon\delta}\right]$. Thus, except when E_- is much smaller than E_+ or $E_\parallel$, J_- is much larger than J_+ and $J_\parallel$.

We now turn to Maxwell's equations. In the resonance layer we replace $\tilde{\underset{\sim}{\nabla}}_\perp$ by $\underset{\sim}{k}_\perp$ and we find easily to leading order

$$\frac{i}{2}(\delta/\varepsilon)^{1/2}\frac{\partial}{\partial\xi'}\left(E_+k_- + E_-k_+\right) + \left(k_\perp^2 - 1\right)E_\parallel = -\left(\omega_{pe}^2/\omega\right)E_\parallel \quad , \tag{2.31}$$

$$-(\delta/\varepsilon)\left(\frac{\partial}{\partial\xi'}\right)^2E_+ + ik_+(\delta/\varepsilon)^{1/2}\frac{\partial}{\partial\xi'}E_\parallel + E_+\left(\frac{1}{2}k_\perp^2 - 1\right) - \frac{1}{2}k_+^2E_-$$

$$= -\frac{\omega_{pe}^2}{\omega(\omega + \Omega_{ce})}E_+ \quad , \tag{2.32}$$

$$-\left(\delta/\varepsilon\right)^2\left(\frac{\partial}{\partial\xi'}\right)^2E_- + ik_-(\delta/\varepsilon)^{1/2}\frac{\partial}{\partial\xi'}E_\parallel + E_-\left(\frac{1}{2}k_\perp^2 - 1\right) - \frac{1}{2}k_-^2E_+ = \frac{-iJ_-}{\omega} \ . \tag{2.33}$$

We have omitted in (2.31)-(2.33) all terms involving spatial derivatives of equilibrium quantities.

The system (2.31)-(2.33) simplifies considerably in the limit of small $k_\perp$. Then Eq. (2.31) describes electron plasma oscillations and Eqs. (2.32) and (2.33) decouple to give the ordinary mode and extraordinary mode, respectively,

$$\left(\frac{\delta}{\varepsilon}\right)\frac{\partial^2E_+}{\partial\xi'^2} + \left[1 - \frac{\omega_{pe}{}^2}{\omega(\omega + \Omega_{ce})}\right]E_+ = 0 \text{ (ordinary mode)} \quad , \tag{2.34a}$$

and

$$\left(\frac{\delta}{\varepsilon}\right)\frac{\partial^2E_-}{\partial\xi'^2} + E_- = -\frac{i}{\omega}J_- \text{ (extraordinary mode)} \quad . \tag{2.34b}$$

To this order, ordinary mode waves propagating nearly parallel to the magnetic field are completely unaffected by finite temperature. For

arbitrary $k_\perp$ the system (2.31)-(2.33) has two distinct forms depending on whether δ/ε is O(1) or large. In either case we may solve (2.31) for $E_\parallel$ to obtain

$$E_\parallel = \frac{\frac{1}{2}i\left(\frac{\delta}{\varepsilon}\right)^{1/2} \frac{\partial}{\partial\xi'}\left(k_+E_- + k_-E_+\right)}{1 - k_\perp^2 - \omega_{pe}^2/\omega^2} \quad . \tag{2.35}$$

When δ/ε is large, we infer from (2.32)

$$E_+ = \frac{-\frac{1}{2}\left(E_+k_- + E_-k_+\right)k_+}{1 - k_\perp^2 - \omega_{pe}^2/\omega^2} \ , \tag{2.36}$$

which we may solve for E_+ and finally substitute into (2.33) to obtain

$$\frac{\left(\frac{\partial}{\partial\xi'}\right)^2 E_-\left(1 - \omega^2{}_{pe}/\omega^2\right)}{1 - \omega_{pe}^2/\omega^2 - \frac{1}{2}k_\perp^2} = \kappa J\left(\xi'\right) \ , \tag{2.37}$$

where

$$J(\xi') = i\int u_\perp du_\perp \ du_\parallel \ d\phi \frac{G(u)}{u_\parallel} \int_{-\infty \mathrm{sgn}(u_\parallel)}^{\xi'} d\xi \ E_-(\xi)\exp\left[\frac{i(\xi'^2 - \xi^2)}{u_\parallel}\right] \tag{2.38}$$

and

$$\kappa\delta/\varepsilon = \left(\frac{1}{\delta\varepsilon}\right)^{1/2} \frac{\omega_{pe}^2}{\Omega_{ce}^2} \ , \tag{2.39}$$

so that

$$\delta^3 = \varepsilon\left(\omega_{pe}^2/\Omega_{ce}^2\right)^2/\kappa^2 \ . \tag{2.40}$$

Note that Eq. (2.37) reduces to (2.34b) as $\kappa_\perp \to 0$. The condition for the validity of the approximations is δ/ε large, or

$$\omega_{pe}^2/\Omega_{ce}^2 > \varepsilon\kappa \ , \tag{2.41}$$

and κ is a dimensionless constant of order one.

When δ/ε is of order one in δ or ε, we may still employ (2.35), but we must reexamine (2.32) and (2.33). We see that the left-hand side of (2.33) is nominally of order one while the right-hand side of (2.33) is of order $(\omega_{pe}^2/\Omega_{ce}^2)E_-/(\varepsilon\delta)^{1/2}$. Thus, in order that both sides of (2.33) be of the same order of magnitude, we require that

$$\delta/\varepsilon = L = O(1) \ , \quad \frac{\omega_{pe}^2}{\Omega_{ce}^2} = \kappa L\sqrt{\varepsilon\delta} = O(\varepsilon) = O(\delta) \ . \tag{2.42}$$

Clearly (2.42) implies that the density is low. The system (2.32) and (2.33), after substitution of (2.35), then reduces in lowest order to

$$\frac{-L\left(\frac{\partial}{\partial\xi'}\right)^2\left[\left(1 - \frac{1}{2}k_\perp^2\right)E_+ + \frac{1}{2}k_+^2E_-\right]}{\left(1 - k_\perp^2\right) + E_+\left(\frac{1}{2}k_\perp^2 - 1\right) - \frac{1}{2}k_+^2E_-} = 0 \ , \tag{2.43}$$

$$\frac{-L\left(\frac{\partial}{\partial\xi'}\right)^2\left[\frac{1}{2}k_-^2E_+ + \left(1 - \frac{1}{2}k_\perp^2\right)E_-\right]}{\left(1 - \kappa_\perp^2\right) - \frac{1}{2}k_-^2E_+ + \left(\frac{1}{2}k_\perp^2 - 1\right)E_+} = -\kappa LJ(\xi') \ , \tag{2.44}$$

and again $J(\xi')$ is given by (2.38).

The system (2.43) and (2.44) has two distinct classes of solutions corresponding to the usual ordinary (O) and extraordinary (E) modes of propagation. For the O mode, $E_{\|} = 0$ and E_+ is given by (2.43) [or (2.44)] with $E_- = 0$. For the E mode, both E_+ and E_- are nonzero while E_- is given by the result of eliminating E_+ from (2.43) and (2.44):

$$L\left(\frac{\partial}{\partial\xi'}\right)^2E_- + \left(1 - k_\perp^2\right)E_- = \left(1 - \frac{1}{2}\ k_\perp^2\right)\kappa LJ\left(\xi'\right) \ , \tag{2.45}$$

while E_+ is given by (2.43) once E_- is known. For either X or O modes, $E_{\|}$ is given by (2.35). The O mode is unaffected by the resonance and we do not study it further.

In summary, in higher density systems E_- is given by (2.37) while δ and ε are constrained by Eqs. (2.40) and (2.41), while in lower density systems E_- is given by (2.45) and the physical constraints are (2.42).

3. ANALYSIS OF THE INTEGRAL EQUATIONS

In this section we examine the integrodifferential equations for the high density, (2.37), and low density, (2.45), cases. We show that the cold plasma model gives many, but not all, of the properties of the solutions of (2.37) and (2.45). We show that for the high density case

a wave incident from the high field side is totally absorbed. That is, no wave reflection occurs at resonance. We present in Sec. 4 the results of numerical solutions of this system given electric field, energy flux, and energy absorption profiles for different cases. For the low density case we show that a wave incident from the high field side suffers no wave reflection but is partially absorbed in and partially transmitted through the resonance layer. The transmission coefficient is found to be exactly the same as in the cold plasma model analysis of Budden tunnelling.[2] These results are proved with some precision. In the low density case and for waves incident from the low field side, our method of analysis fails. But subject to far more stringent hypotheses and in the spirit of a purely formal proof, we show that the transmission coefficient for waves incident from the low field side equals the transmission coefficient in the case of high field side incidence. We are unable to give any information on the reflection coefficient. The equality of the two transmission coefficients is also a cold plasma model result. Similar results on the transmission and reflection coefficients were found at fundamental resonance in a perpendicularly stratified medium.[6]

The method of proof we employ is an extension of the techniques used in the case of a perpendicularly stratified medium.[6] We recast the integrodifferential equation as an integral equation in which we compare the solution to that in the cold plasma model. We extend the equations into the complex plane under the assumption that the solution is extendible in the complex plane in a particular way. Finally, we show that within a particular class of functions the integral equation has a unique solution. Further, this solution has an asymptotic expansion valid for large argument which matches the solution of the problem in

the cold plasma model. The method works only for waves incident from the high field side as only this solution satisfies our hypotheses. This analysis shows us that for high field side wave incidence, no wave is reflected and the transmitted wave (which exists only in the low density case) is the same as in the cold plasma model. In the low density case of low field side incidence, we obtain the transmission coefficient from a generalized Wronskian relation. We consider reduced distribution functions which are analytic in $u_{||}$ in appropriate domains and which satisfy other hypotheses. A wide class of distribution functions is included, but the assumption is restrictive and it is critical. Without it we cannot obtain the results presented here.

Before we proceed to the two distinct integrodifferential equations, we obtain a few general properties of our system applicable in either case. We recall that our equations possess solutions that are analytic in the domain $\mathrm{Im}\{\omega\} < 0$. In view of the definition (2.25), we see that we may expect our solutions to be analytic in $\mathrm{Im}\{\xi\} > 0$. Since the solutions must tend to zero as $\mathrm{Im}\{\omega\} \to -\infty$, it is tempting to assume a comparable property of the solutions as $\mathrm{Im}\{\xi\} \to +\infty$. This property is, however, false. The parameter ω occurs in the integrodifferential equation in other places besides the combination (2.25). Thus, $\mathrm{Im}\{\omega\} \to -\infty$ is not equivalent to $\mathrm{Im}\{\xi\} \to +\infty$. Nonetheless our solutions are analtyic in $\mathrm{Im}\{\xi\} > 0$, and our method of proof applies only to those solutions (if any) which tend to zero as $\mathrm{Im}\{\xi\} \to +\infty$. In other problems[6] where we have calculated numerically those solutions which are large as $\mathrm{Im}\{\xi\} \to +\infty$, we have found that they are not approximately given by the cold plasma solutions. Thus, we suspect that with the analysis and the Wronskian relation we have extracted the maximum analytic information possible.

We first examine the integral kernel (2.38) that occurs in both problems. After we perform the $u_\perp$ and ϕ integrations we may define a reduced distribution function

$$g(u_\parallel) = \int G(u_\parallel, u_\perp)u_\perp du_\perp d\phi = g(-u_\parallel) \tag{3.1}$$

normalized and scaled so that

$$\int_{-\infty}^{\infty} g(u_\parallel)du_\parallel = \int_{-\infty}^{\infty} u_\parallel^2 g(u_\parallel)du_\parallel = 1 \ . \tag{3.2}$$

The basic integral kernel then becomes

$$J(\xi') = MoE_- = i \int_{-\infty}^{\infty} g(u_\parallel)\frac{du_\parallel}{u_\parallel} \int_{-\infty\,\mathrm{sgn}(u_\parallel)}^{\xi} d\xi E_-(\xi)\exp\left[i(\xi^2 - \xi^2)/u_\parallel\right] \ , \tag{3.3}$$

or

$$MoE_- = i \int_{-\infty}^{\xi'} d\xi E_-(\xi)\int_0^{\infty} du_\parallel \left[g(u_\parallel)/u_\parallel\right]\exp\left[i(\xi'^2 - \xi^2)/u_\parallel\right]$$

$$+ i\int_{\xi'}^{\infty} d\xi E_-(\xi) \int_0^{\infty} du_\parallel \left[g(u_\parallel)/u_\parallel\right]\exp\left[-i(\xi'^2 - \xi^2)/u_\parallel\right] \ . \tag{3.4}$$

On a purely formal basis, if we integrate by parts two times with respect to ξ we find

$$\mathrm{Mo}E_- = -E_-/2\xi' - (i/4)\int_{-\infty}^{\xi} d\xi\left\{\left[E(\xi)/\xi\right]'/\xi\right\}'\int_0^{\infty} u_{\|}g(u_{\|})du_{\|}\exp\left[i(\xi^2 - \xi^2)/u_{\|}\right]$$

$$-(i/4)\int_{\xi}^{\infty} d\xi\left\{\left[E(\xi)/\xi\right]'/\xi\right\}'\int_0^{\infty} u_{\|}g(u_{\|})du_{\|}\exp\left[-i(\xi'^2 - \xi^2)/u_{\|}\right] . \tag{3.5}$$

For (3.5) to be valid we require only that $E_-(\xi')$ be sufficiently differentiable that the function and its derivatives do not grow too rapidly at infinity and that the integrands be defined at all points on the path of integration. We shall shortly extend the path of ξ integration into the complex plane and restrict the class of functions $E_-(\xi)$ so as to assure the validity of (3.5). We note in passing that the first term on the right-hand side of (3.5) gives rise to the usual cold plasma conductivity.

The properties of the integral kernel M are largely determined by the properties of the functions

$$I_n(\lambda) = \int_0^{\infty} du_{\|}u_{\|}^n g(u_{\|})\exp(i\lambda/u_{\|}) \tag{3.6}$$

for $n = \pm 1$. For a general smooth, but not necessarily analytic, distribution function $I_n(\lambda)$ possesses an analytic continuation into $\mathrm{Im}\{\lambda\} > 0$ and for large $|\lambda|$ and $n \geq 1$, and if $g(u_{\|})$ has N integrable derivatives, then

$$|I_n(\lambda)| \leq K_N/|\lambda|^N . \tag{3.7}$$

The estimate (3.7) and analytic continuation into $\mathrm{Im}\{\lambda\} > 0$ are not adequate to complete our proof. For a Maxwellian distribution,

$g(u_{\|}) = (1/\sqrt{2\pi})\exp(-\frac{1}{2}\, u_{\|}^2)$, we may obtain much stronger estimates. In this case it is easy to show directly from (3.6) that for any $\delta > 0$, $I_n(\lambda)$ is analytic in

$$|\arg \lambda - \pi/2| = |\arg(-i\lambda)| < \frac{3\pi}{4} - \delta \tag{3.8}$$

and in that sector and for $|\lambda| \geq 1$,

$$|I_n(\lambda)| < \alpha|\exp\left[-\beta(-i\lambda)^{2/3}\right]| \ , \tag{3.9}$$

where α and β are functions of n and δ. In fact, $I_n(\lambda)$ is analytic in a larger domain, but the estimates (3.8) and (3.9) are adequate for our purposes. If we were to multiply the Maxwellian by any given polynomial in $(u_{\|})$, (3.8) and (3.9) would still hold with new values of α and β. In our proofs we assume that (3.8) and (3.9) hold. With no great additional effort we could consider distribution functions $g(u_{\|})$, which are analytic and which for large $|u_{\|}|$ satisfy $g(u_{\|}) \sim p(u_{\|})\exp\left(-|u_{\|}|^{1+\gamma}\right)$, $\gamma > 0$, and $p(u_{\|})$ a polynomial in $u_{\|}$. In this case, $I_n(\lambda)$ would be analytic in a domain $|\arg(-i\lambda)| < (\pi/2) + \delta'$ for some $\delta' > 0$ and would satisfy an estimate there of the form (3.9) with $(-i\lambda)^{2/3}$ replaced by $(-i\lambda)^{(\gamma+1)/(\gamma+2)}$. We restrict ourselves to Maxwellians and the estimates (3.8) and (3.9) although some limited generalization is possible.

In terms of the function $I_n(\lambda)$ just introduced, if we change the variable of integration in (3.4) and (3.5) from ξ to $x = \xi - \xi'$ and for simplicity of notation we replace ξ' by ζ, we obtain

$$\mathrm{MoE}_- = i \int_{-\infty}^{0} dx\, E_-(x + \zeta) I_{-1}(-x^2 - 2x\zeta)$$

$$+ i \int_{0}^{+\infty} dx\, E_-(x + \zeta) I_{-1}(x^2 + 2x\zeta) \quad , \tag{3.10}$$

and after formal integration by parts,

$$\mathrm{MoE}_- = \frac{-E(\zeta)}{(2\zeta)} - (i/4) \int_{-\infty}^{0} dx \left[\frac{E_-(x + \zeta)}{x + \zeta}\right]' I_1(-x^2 - 2x\zeta)$$

$$-(i/4) \int_{0}^{\infty} dx \left\{\left[\frac{E_-(x + \zeta)}{x + \zeta}\right]' / (x + \zeta)\right\}' / I_1(x^2 + 2x\zeta) \ . \tag{3.11}$$

If $E_-(\zeta)$ is analytic in the upper half-plane and grows no faster than a polynomial in ζ at infinity, then (3.10) provides an analytic continuation of the operator M for complex ζ and (3.10) is justified in $\mathrm{Im}\{\zeta\} > 0$. We next address a change in the path of x integration in (3.10) and (3.11).

We have examined the analytic functions $I_n(\lambda)$, but we see that in (3.10) and (3.11) the argument of $I_n(\lambda)$ is the more intricate entity $\pm(x^2 + 2x\zeta)$. In order to apply the estimate (3.9), we must determine the argument of $x^2 + 2x\zeta$. We start by consideration of the simple analytic function

$$\psi(\sigma) = \sigma(\sigma + 2) \ , \tag{3.12}$$

where $\sigma = \sigma_r + i\sigma_i$. We see that on the curves $\sigma_i = 0$ and $\sigma_r = -1$, $\mathrm{Im}\{\psi\} = 0$, while in the curves $(\sigma_r + 1)^2 - \sigma_i^2 = 1$, $\mathrm{Re}\{\psi\} = 0$ (see Fig. 2). In Fig. 2 $\mathrm{Im}\{\psi\}$ changes sign across a dotted line, while $\mathrm{Re}\{\psi\}$

ORNL-DWG 86-2055 FED

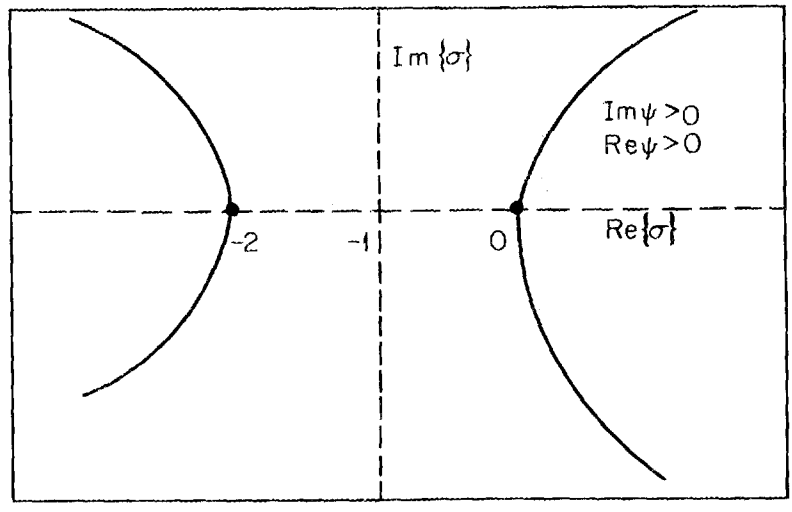

Fig. 2. Contours $\mathrm{Im}\{\psi\} = 0$ and $\mathrm{Re}\{\psi\} = 0$ in the complex σ plane $\psi = \sigma(\sigma + 2)$.

changes sign across a solid line. It is also useful to describe the curves $\arg \psi(\sigma) = \text{const}$, which we give in Fig. 3 for $\mathrm{Re}\{\psi\} > -1$. The curves for $\mathrm{Re}\{\sigma\} < -1$ are the mirror image of those shown. The curves $\arg \psi = \text{const}$ are all rectangular hyperbolas given by the relation

$$2\sigma_i(\sigma_r + 1) = \left\{\tan\left[\arg(\psi)\right]\right\}(\sigma_r^2 - \sigma_i^2 + 2\sigma_r) \quad .$$

It is easy to show that for any value of $\tan[\arg(\psi)]$ the corresponding rectangular hyperbolas are asymptotic to lines which make angles of $\arg(\psi) \pm k\pi$ and $\arg(\psi) \pm (k + 1/2)\pi$ with the real axis.

The argument of $I_\pm$ may be expressed as

$$\phi(x, \zeta) = \zeta^2\left[(x/\zeta)^2 + 2(x/\zeta)\right] ,$$

ORNL-DWG 86-2053 FED

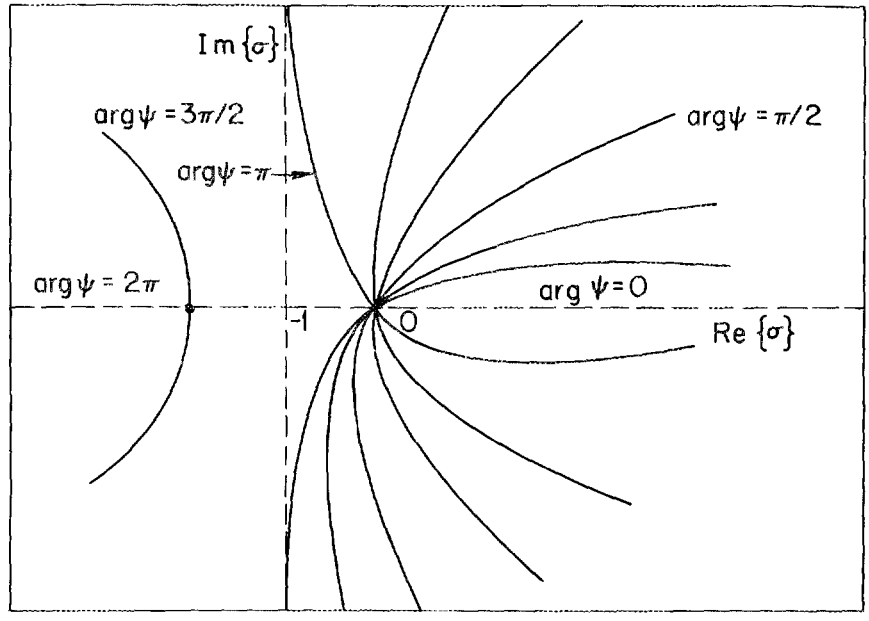

Fig. 3. Contours of arg(ϕ) = const in complex σ plane.

so that

$$\arg \phi(x, \zeta) = 2 \arg \zeta + \arg\left[\psi(x/\zeta)\right] . \tag{3.12}$$

Thus, for any $\zeta = |\zeta|\exp[i \arg(\zeta)]$, in order to obtain the curves of constant phase of $\phi(x, \zeta)$ in the complex x plane, we add 2 arg(ζ) to the phase of ψ as given in Fig. 3 and we rotate Fig. 3 in a positive, (counterclockwise) sense by an angle equal to arg ζ. For ζ real and positive, Fig. 3 applies. For ζ pure imaginary, the corresponding figure (with only critical curves shown) is given in Fig. 4.

For ζ real and negative, we show the critical lines of constant phase in Fig. 5. In Figs. 3 through 5 we have adjusted the phase such that for $|x|$ large arg(ϕ) ~ 2 arg x.

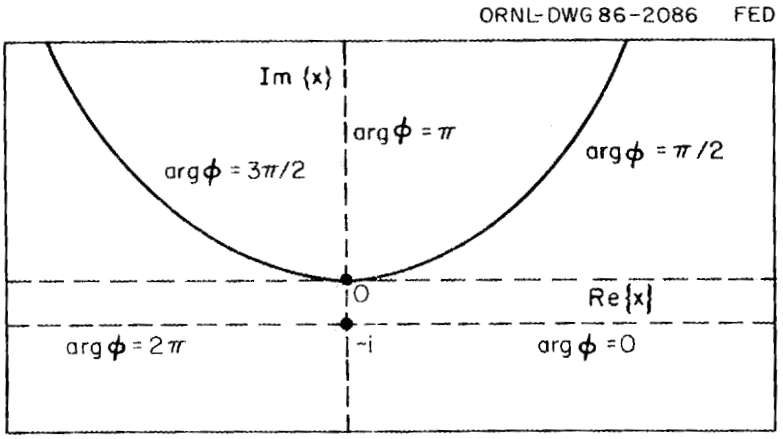

Fig. 4. Contours of arg(ϕ) = const in complex x plane, ζ is pure imaginary.

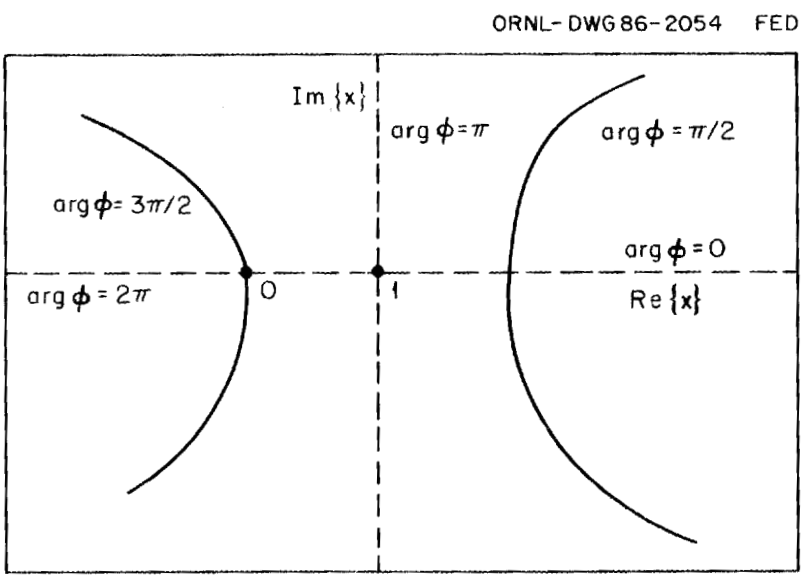

Fig. 5. Contours of arg(ϕ) = const in complex x plane, ζ real and negative.

We now return to the consideration of the integral kernel given by (3.10). Since $I_{\pm 1}(\lambda)$ is exponentially bounded by (3.9) in the sector $-\pi/4 < \arg \lambda < 5\pi/4$, it is easy to see from Figs. 3 through 5 that for all ζ, $\mathrm{Im}\{\zeta\} \geq 0$ it is possible to deform the integrals in (3.10) into the upper half-plane and yet maintain the argument $\pm 2x(x + \zeta)$ in the appropriate sector. In this process each integral in (3.10) or (3.11) must be treated separately, and each integral yields a distinct contour of integration. Once we have moved the paths of integration into the upper half-plane, it is then trivial to integrate by parts twice and obtain (3.11) as the expression for the integral operator, where it is understood that the path of integration is in the upper half-plane and on a contour in which $\arg[\pm x(x + 2\zeta)]$ is uniformly in the correct sector and the path of integration is such that

$$|x + \zeta| \geq \tilde{k}|\zeta| \quad . \tag{3.12a}$$

Additionally, on the paths of integration we may also assume

$$|x(x + 2\zeta)| \geq \tilde{k}|x||\zeta| \quad . \tag{3.12b}$$

Thus, on the paths of integration

$$|I_{\pm 1}| \leq \alpha \exp\left(-\beta|x|^{2/3}|\zeta|^{2/3}\right) \tag{3.13}$$

for some $\tilde{k}$ for all x and all ζ, $|\zeta| \geq 1$.

We may finally recast our integrodifferential equation in the form

$$E'' + \left[a + b/(2\zeta)\right]E = bM_1 oE \ , \tag{3.14}$$

where we have replaced $E_-(\zeta)$ by $E(\zeta)$ and we have defined

$$MoE = bE/(2\zeta) + M_1 oE \quad , \tag{3.15}$$

and

$$a = (1 - k_\perp^2)(\varepsilon/\delta) \quad , \tag{3.16}$$

$$b = \left[\left(1 - \omega_{pe}^2/\Omega_{ce}^2 - \frac{1}{2}k_\perp^2\right)/\left(1 - \omega_{pe}^2/\Omega_{ce}^2\right)\right]\left(\omega_{pe}^2/\Omega_{ce}^2\right)\varepsilon^{1/2}\delta^{-3/2} \quad . \tag{3.17a}$$

In the high density case, a is set to zero since ε/δ tends to zero, while in the low density case, (ε/δ) is $O(1)$ and $\omega_{pe}^2/\Omega_{ce}^2$ is small so that

$$b = \left(1 - \frac{1}{2}k_\perp^2\right)\left[\omega_{pe}^2/(\Omega_{ce}^2\delta)\right]\left(\varepsilon/\delta\right)^{1/2} \tag{3.17b}$$

and each factor in (3.17b) is $O(1)$. In (3.14)-(3.17) we have a unified form for both the high density and low density cases. We now examine (3.14) in $\mathrm{Im}\{\zeta\} \geq 0$.

Our proofs require that we distinguish the two cases and we treat first the high density case in which $a = 0$ and $b > 0$. Two linearly independent solutions of $u'' + b/(2\zeta)u = 0$ are $\zeta^{1/2}H_1^{(1)}(\sqrt{2b\zeta})$ and $\zeta^{1/2}H_1^{(2)}(\sqrt{2b\zeta})$. Clearly the first solution is exponentially small in ζ for $\pi \geq \arg\zeta > 0$, while the second solution is exponentially large there. We set

$$u_1(\zeta) = \zeta^{1/2}H_1^{(1)}\left(\sqrt{2b\zeta}\right) \tag{3.18a}$$

and

$$u_2(\zeta) = f\zeta^{1/2}H_1^{(2)}\left(\sqrt{2b\zeta}\right) , \tag{3.18b}$$

where we select f so that the Wronskian of u_1 and u_2 is one. An integral equation equivalent to the differential equation (3.14) is

$$E = u_1(\zeta) + bu_1(\zeta)\int_\zeta^\infty d\zeta' u_2(\zeta')M_1 oE - bu_2(\zeta)\int_\zeta^\infty d\zeta' u_1(\zeta')M_1 oE \quad . \tag{3.19}$$

We show that the integral equation (3.19) is well defined and that for large $\zeta E(\zeta) = u_1(\zeta)[1 + o(1)]$. We will then have shown that a wave incident from the right-hand (high field) side is totally absorbed, since $u_1(\zeta)$ describes such a wave. Since $u_2(\zeta)$ is exponentially large in the upper half-plane, it is not at all obvious that the integrals in (3.19) are well defined. We must select a domain in the upper half-plane, show that for all ζ there the equation is defined, and then show that Picard iteration converges. The choice of proper paths of integration in (3.11) and in (3.19) is essential in this activity.

We are finally ready to specify our class of functions. Since we expect $E(\zeta)$ to behave asymptotically like $u_1(\zeta)$, we expect for (ζ) large

$$E(\zeta) \sim \text{const}\ \sqrt{\zeta}\ \exp(i\sqrt{2b\zeta}) \quad .$$

The integral operator $M_1 oE$ involves not only the function E but also its first two derivatives. Thus, we define the function norm

$$||E(\zeta)|| = \sup_{\zeta\varepsilon D}\left\{\left[|E(\zeta)/\sqrt{\zeta}| + |E'(\zeta)/\zeta^{3/2}| + |E''(\zeta)/\zeta^{5/2}|\right]|e^{-i\sqrt{2b\zeta}}|\right\} \quad , \tag{3.20}$$

where $E(\zeta)$ is analytic in the upper half-plane and D is as yet an unspecified subset of the upper half-plane. We prove convergence of Picard iteration for (3.19) only for $|\zeta| > R$ for some R. Further, we require that each point in D have the two contours of integration in the definition of M_1 in D as well. Thus, we have a domain whose shape is indicated in Fig. 6. We finally pick R when we complete our estimates.

Suppose $E(\zeta)$ has finite norm according to (3.20), then for some $C_1 > 0$

$$\left|\left[M_1 o E(\zeta)\right]\left(e^{-i\sqrt{2b}\zeta}\right)/\sqrt{\zeta}\right| \leq \left(C_1/|\zeta|^{7/2}\right)||E||$$

$$\int |dx| \exp\left[|\sqrt{2b}(x+\zeta) - \sqrt{2b}\zeta| - \beta|x|^{2/3}|\zeta|^{2/3}\right] . \quad (3.21)$$

If we set

$$\chi(x) = |\sqrt{2b}(x+\zeta) - \sqrt{2b}\zeta| - \beta|x|^{2/3}|\zeta|^{2/3} \quad ,$$

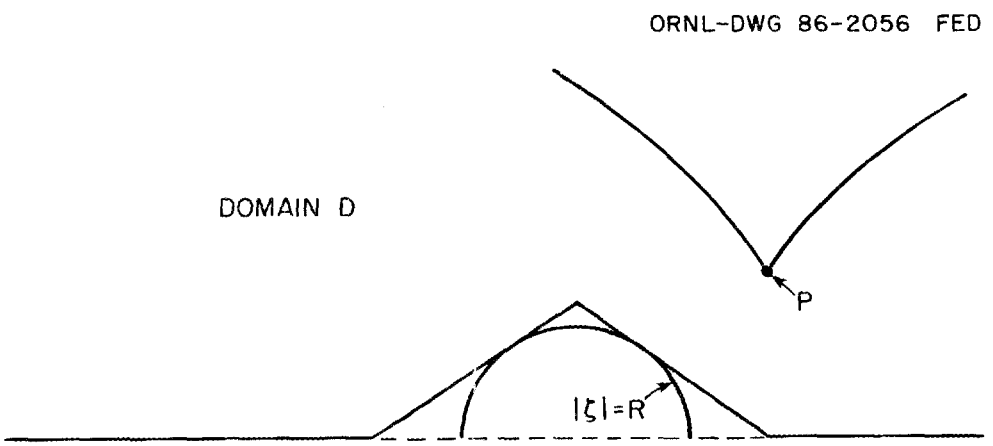

Fig. 6. Domain of definition of M_1 in complex ζ plane. Domain consists of all points P having two convergent contours of integration, each point of which lies outside $|\zeta| \leq R$.

we see that

$$X(x) = |2b\zeta|^{1/2}\left(|\sqrt{1+u}-1| - \beta'|u|^{2/3}|\zeta|^{5/6}\right) ,$$

where $\beta' = \beta/\sqrt{2b}$ and $u = x/\zeta$. Since $|\sqrt{1+u}-1| \leq 2|u|^{1/2}$ we see that for $|\zeta|$ large enough, or R large enough, the integral in (3.21) exists and is clearly independent of E, so that

$$|[M_1 oE(\zeta)]\left(e^{-i\sqrt{2b}\zeta}\right)/\sqrt{\zeta}| \leq C_2||E||/|\zeta|^{7/2} . \tag{3.22}$$

We now return to the integral equation (3.19) and we select the path of integration to be from ζ to $\zeta + i\infty$ along a ray parallel to the imaginary axis. It now follows that

$$|\int_{\zeta}^{i\infty} d\zeta' u_2(\zeta')M_1 oE(\zeta')| \leq C_3||E||/|\zeta|^{3/2} \tag{3.23}$$

and

$$|\int_{\zeta}^{i\infty} d\zeta' u_1(\zeta')M_1 oE(\zeta')| \leq C_4||E|| \; |\left[\exp(2i\sqrt{2b}\zeta)\right]/\zeta^{3/2}| . \tag{3.24}$$

If we finally rewrite the integral equation (3.19) as

$$E(\zeta) = u_1(\zeta) + NoE , \tag{3.25}$$

then it follows trivially from the definitions and from (3.23) and (3.24) that

$$||NoE|| \leq C_5||E||/|\zeta|^{3/2} . \tag{3.26}$$

Hence for R large enough that $C_5/R^{3/2} < 1$, N defines a contractive mapping and (3.25) possesses a unique solution in the class of functions

of finite norm given by (3.20). The estimate (3.26) further indicates that for $|\zeta|$ large the solution obeys

$$E(\zeta) = u_1(\zeta)\left[1 + 0\left(|\zeta|^{-3/2}\right)\right] , \tag{3.27}$$

and (3.27) applies uniformly in D. Thus, we have shown that the incoming wave is totally absorbed without any wave reflection.

We now turn to the low density case corresponding to the integrodifferential equation given by (3.14) with both a and b nonzero. Our aim is to recast this equation into a pure integral equation of the form (3.19). To this end we must select the functions $u_1(\zeta)$ and $u_2(\zeta)$, which we take in this case to be solutions of a special case of the confluent hypergeometric equation

$$u'' + \left[a + b/(2\zeta)\right] u = 0 ,$$

for which two linearly independent solutions are (see Ref. 7)

$$u_{\pm} = W_{\pm\mu,"2}\left(\mp 2i\sqrt{a}\ \zeta\right) ,$$

where

$$\mu = ib/(4\sqrt{a}) . \tag{3.28}$$

Thus we take

$$u_1 = W_{+\mu,"2}\left(-2i\sqrt{a}\zeta\right) , \tag{3.29}$$

for which the asymptotic expansion valid in $\mathrm{Im}\{\zeta\} \geq 0$ is

$$u_1 = \left\{\exp\left[i\sqrt{a}\zeta + \mu \log(-2i\sqrt{a}\zeta)\right]\right\}\left[1 + 0(1/\zeta)\right] . \tag{3.30}$$

We note that the choice of functions here is different from that in Ref. (7), since our functions are analytic in the upper half-plane instead of being analytic in the lower half-plane as in Ref. (7). The solution u_1 is exponentially small as $\mathrm{Im}\{\zeta\} \to +\infty$.

We take as the second solution

$$u_2 = gW_{-\mu,1/2}(2i\sqrt{a}\zeta) \ , \tag{3.31}$$

where g is chosen so that the Wronskian of u_1 and u_2 is one. The obvious range of validity of asymptotic expansions of $W_{k,m}(z)$ is the sector $|\arg(z)| < \pi - \delta$, but the standard integral representations of these functions indicate that the range of validity of these expansions is, in fact, $|\arg(z)| < \frac{3\pi}{2} - \delta$. The lines $\arg(z) = \pm\frac{3\pi}{2}$ are Stokes lines across which the expansions are discontinuous. Thus, in $0 \leq \arg \zeta \leq \pi - \zeta$

$$u_2 = g\left\{\exp\left[-i\sqrt{a}\zeta - \mu \log(2i\sqrt{a}\zeta)\right]\right\}\left[1 + O(1/\zeta)\right] \quad . \tag{3.32}$$

If we duplicate the analysis found in Ref. (7) concerning analytic continuation of Whittaker functions, we find that in $\pi/2 + \delta < \arg \zeta \leq \pi$

$$u_2 = g\left\{\exp\left[-i\sqrt{a}\zeta - \mu \log(2i\sqrt{a}\zeta)\right]\right\}\left[1 + O(1/\zeta)\right]$$

$$+ h\left\{\exp\left[i\sqrt{a}\zeta + \mu \log(-2i\sqrt{a}\zeta)\right]\right\}\left[1 + O(1/\zeta)\right] \ , \tag{3.33}$$

where the explicit value of h is of no interest here. Except in the neighborhood of the negative real axis, the term proportional to h is exponentially small compared wtih the first term. On the negative real axis, both terms are comparable.

With $u_1(\zeta)$ and $u_2(\zeta)$ defined by (3.29) and (3.31), we may rewrite the equation (3.14) in the form (3.19). For functions analytic in the upper half-plane, we define

$$||E|| = \sup_{\zeta\varepsilon D} \left\{ \left[|E(z)| + |E'(\zeta)| + |E''(\zeta)| \; |\exp(-i\sqrt{a}\zeta)| \right] \right\} . \tag{3.34}$$

We can now easily parallel the first proof. Corresponding to (3.22), we now find, far more easily,

$$|(M_1 o E)e^{-i\sqrt{a}\zeta}| \leq \bar{c}_2 ||E|| / |\zeta|^2 \quad , \tag{3.35}$$

so that

$$|\int_{\zeta}^{i\infty} d\xi' M_1 o E u_2(\xi')| \leq \bar{c}_3 ||E|| / |\zeta| \tag{3.36}$$

and

$$|\int_{\zeta}^{i\infty} d\xi' M_1 o E u_1(\xi')| \leq \bar{c}_4 ||E|| \; |e^{2i\sqrt{a}\zeta}| / |\zeta| \; , \tag{3.37}$$

where (3.36) and (3.37) correspond to (3.23) and (3.24). The integral operator N for this problem, see (3.35), then satisfies the estimates

$$||NoE|| \leq \bar{c}_5 ||E|| / |\zeta| \quad . \tag{3.38}$$

Thus, for $R > \bar{c}_5$, N generates a contractive mapping. Within the class of functions with finite norm according to (3.34), the integrodifferential equation has a unique solution and for this solution

$$E = u_1(\zeta)\left[1 + O(1/|\zeta|)\right] . \tag{3.39}$$

Now the solution u_1 corresponds to a wave incident from the high field side with no reflected wave and with transmitted amplitude $T = \exp\left[-b\pi/(2\sqrt{a})\right]$, exactly as in cold plasma theory and geometrical optics. The energy absorption is $1 - T$, and the problem is essentially what one would find in a cold plasma model.

We next turn to the case of waves incident from the low field side. We cannot apply the previous analysis since the solution must have the asymptotic form of u_2, which is exponentially large in the upper half-plane. In this case we apply a Wronskian relation, and we work on the real axis only. We must hypothesize rather strong conditions on the solutions. We believe the hypotheses are reasonable, but we cannot be sure that the hypotheses hold. For two solutions of the integrodifferential equation (3.14), $E(\zeta)$ and $F(\zeta)$, we hypothesize

$$I = \int_{-\infty}^{\infty} d\zeta\ F(\zeta) MoE(\zeta) \tag{3.40}$$

exists and may be treated without concern for convergence problems. We may write

$$MoE = i \int_{-\zeta}^{\zeta} dx\ E(x) I_{-1}(\zeta^2 - x^2) + i \int_{\zeta}^{\infty} dx\ E(x) I_{-1}(x^2 - \zeta^2) \quad ,$$

and it is then trivial to show that

$$I = \int_{-\infty}^{\infty} d\zeta\ E(\zeta) MoF(\zeta) \quad . \tag{3.41}$$

Since we have the estimate on M_1 (3.35) it is quite likely that the interchange of integrations implied to obtain (3.41) is valid. If we return to the differential equation (3.14), we readily conclude

$$\left[F(\zeta)E'(\zeta) - F'(\zeta)E(\zeta)\right]' = F(\zeta)MoE(\zeta) - E(\zeta)MoF(\zeta)$$

so that

$$\lim_{\substack{A\to\infty \\ B\to-\infty}} \left[F(A)E'(A) - F'(A)E(A) - F(B)E'(B) + F'(B)E(B)\right] = 0 \quad . \tag{3.42}$$

If we now assume that there is a solution of (3.14) which as $\zeta \to -\infty$ has the expansion

$$F(\zeta) = \left\{\exp\left[-i\sqrt{a}\zeta - \mu \log(2i\sqrt{a}\zeta)\right]\right\}\left[1 + O(1/|\zeta|)\right]$$

$$+ R_L\left\{\exp\left[i\sqrt{a}\zeta + \mu \log(2i\sqrt{a}\zeta)\right]\right\}\left[1 + O(1/|\zeta|)\right] \tag{3.43}$$

while for $\zeta \to +\infty$

$$F(\zeta) = T_L\left\{\exp\left[-i\sqrt{a}\zeta - \mu \log(2i\sqrt{a}\zeta)\right]\right\} 1 + O(1/|\zeta|) \quad , \tag{3.44}$$

and if we apply (3.42) with $E(\zeta)$ as the solution previously obtained for the high field side incidence problem, we conclude

$$T_L = T \quad , \tag{3.45}$$

where T_L is the transmission coefficent for low field side incident waves. We are unable to offer any information concerning R_L, which we believe must be calculated numerically.

4. NUMERICAL COMPUTATION OF STRONGLY DAMPED WAVES IN DENSE PLASMAS

In the case of extraordinary mode waves propagating nearly parallel to the magnetic field or for finite $k_\perp$ with ε and δ satisfying the conditions of Eq. (2.39), the equation for E_- reduces to the simple form

$$\frac{\partial^2 E_-}{\partial \zeta^2} = \kappa J_-(\zeta) \quad , \tag{4.1}$$

where $J(\zeta)$ is given by Eq. (2.38) and κ is given in (2.39). When the unperturbed distribution is Maxwellian, $G(\underline{u}) = \exp(-u^2)/(\pi)^{3/2}$, the velocity space integrals can be performed and the plasma current expressed as a convolution integral

$$\kappa J_-(\zeta) = \int_{-\infty}^{\zeta} d\xi\, E(\xi)\, H(\zeta^2 - \xi^2) + \int_{\zeta}^{\infty} d\xi\, E(\xi)\, H(\xi^2 - \zeta^2) \tag{4.2}$$

where the Green's function $H(x)$ is

$$H(x) = \int_0^{\infty} \frac{du}{u}\, e^{-u^2 - ix/u} \quad . \tag{4.3}$$

The first integral in Eq. (4.2) arises from particles streaming from low field to high field [i.e., $u_\parallel < 0$ in Eq. (2.38)] whereas the second comes from $u_\parallel > 0$.

Before presenting the numerical solution of Eq. (4.1), it is of interest to examine the structure of $H(x)$ and to compare the nonlocal plasma response given by (4.2) to that predicted by local, warm plasma theory. Figure 7 shows the real and imaginary parts of $H(x)$. At $x = 0$

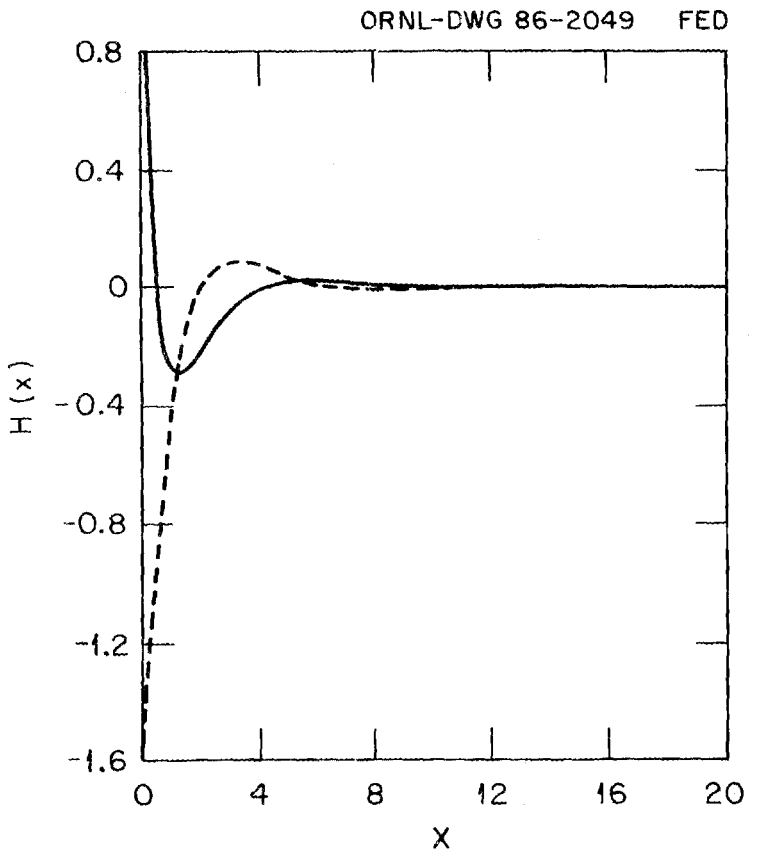

Fig. 7. Real part (solid curve) and imaginary part (dashed curve) of Greens function H(x), Eq. (4.3).

there is a logarithmic singularity [$H(x) \sim -\ln x - 3\gamma/2 - \pi i/2$ as $x \to 0$], and for large x there is an asymptotic expansion of the form

$$H(x) \sim \exp\left[-\frac{3}{4}\, 2^{1/3}(1 + \sqrt{3}i)x^{2/3}\right] \left(\frac{A}{ix}\right)^{1/3} ,$$

which is exponentially damped and rapidly oscillating for large x. Thus the nonlocal contribution to the current is negligible for $|\xi^2 - \zeta^2| \geq 10$. The real part of H gives rise to the dissipative part of the plasma current, the part in phase with $E_{\parallel}$. From Fig. 7 we see that Re{H} is singular near $\xi = \zeta$ and so the dissipation is approximately

local. However, since Re{H} oscillates negative in the approximate range $0.5 < x < 5.0$, it is possible to have local negative dissipation for some electric field profiles. This is actually found to occur in the numerical solutions.

The perturbed plasma current as predicted by local, warm plasma theory in the present scaled variables is obtained by replacing $\partial/\partial\zeta$ by $i\bar{k}$ and treating ζ as a constant parameter in Eq. (2.38). For a Maxwellian distribution, one obtains

$$S_{local}(\zeta) = K \frac{\sqrt{\pi}i}{\bar{k}} Z\left(-\frac{\zeta}{\bar{k}} E_{-}(\zeta)\right) \quad , \tag{4.4}$$

where $Z(x)$ is the plasma dispersion function. We now calculate the perturbed current for an assumed incident wave field of the form

$$E_{-}(\zeta) = \begin{cases} 0 & \zeta < 0 \\ e^{i\bar{k}\zeta} & \zeta \geq 0 \end{cases} \quad . \tag{4.5}$$

Figure 8 shows the real parts of $J(\zeta)$ (solid) and $J_{local}(\zeta)$ (dashed) for an undamped plane wave incident from large ζ $\bar{k}_r = 1.0$, $\bar{k}_i = 0.0$. At large values of ζ, $\zeta \gtrsim 8$ both profiles agree with the cold plasma result, $J \propto E_{-}(\zeta)/\zeta$. For $\zeta \gtrsim 7$ there is a small difference, primarily a phase shift with $J(\zeta)$ lagging J_{local}. However, if one plots the profile of power dissipation, $P_D \propto \mathrm{Re}\{\underset{\sim}{E}^* \cdot \underset{\sim}{J}\}$, shown in Fig. 9, a much more significant difference is seen. Initially the dissipation is negative, $4.5 \lesssim \zeta \lesssim 7$, then the nonlocal dissipation increases more rapidly than the prediction of local theory. If one takes the incident wave to be damped, these features of negative dissipation followed by rapid positive dissipation are increased. This is shown in Fig. 10, where $\bar{k}$ was taken to be $\bar{k} = -2 - 0.5i$. Although the complex $\bar{k}$ was included in

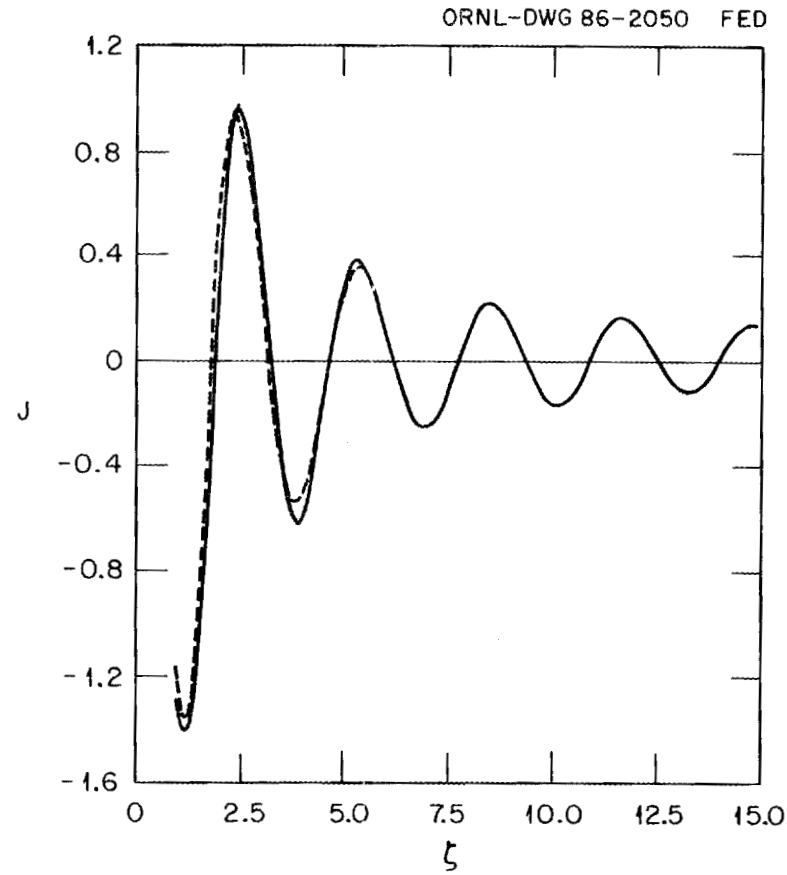

Fig. 8. Real part of nonlocal current profile (solid curve) and local current profile for a specified undamped plane wave electric field.

Eq. (4.4), the shape of $P_{D\ local}(\zeta)$ is almost unchanged by including damping. We conclude therefore that nonlocal effects can be important in determining the perturbed current and that these nonlocal effects are sensitive to the wave field profile in the resonance region.

The numerical solution of the system (4.1)-(4.3) has been carried out in a previous work[5] where the same system appeared in the investigation of ion cyclotron heating in tokamaks. The numerical methods of solution are discussed in detail in that reference.

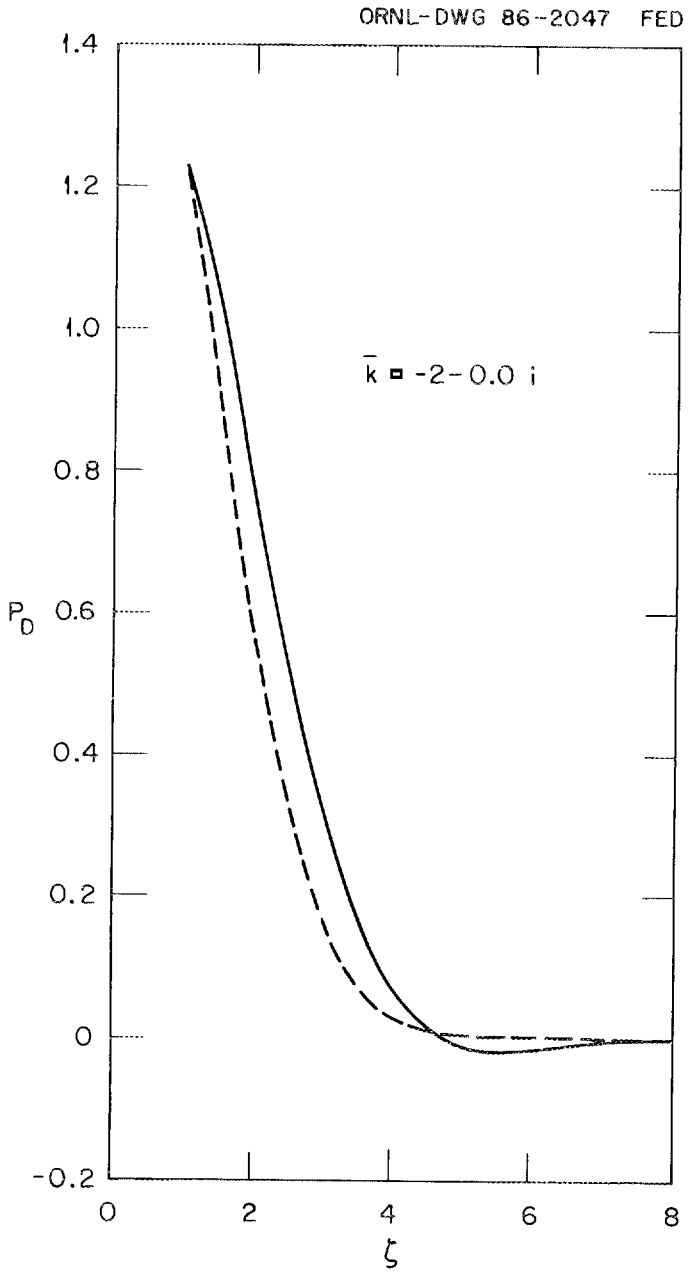

Fig. 9. Power dissipation profile $P_D = \mathrm{Re}\{E^* \cdot J\}$ for nonlocal current response (solid curve) and local current response. $\underline{E}$ is a specified undamped plane wave, $\bar{k} = -2$.

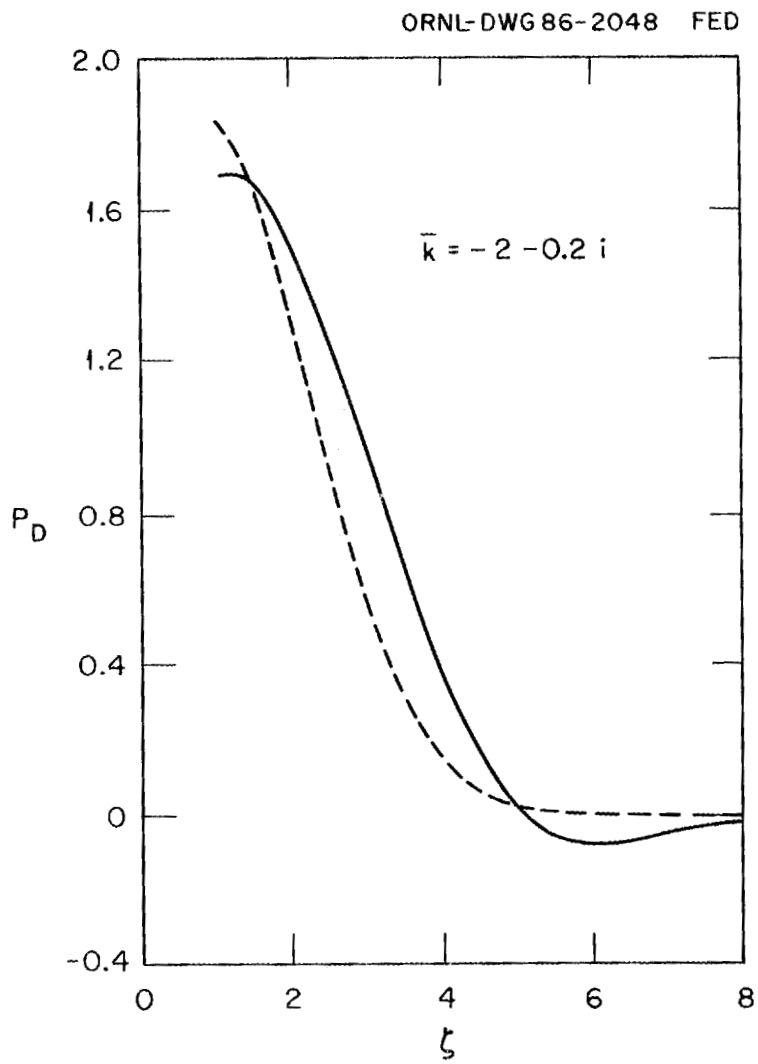

Fig. 10. Similar to Fig. 9 except electric field is specified to be a damped plane wave, k = -2 - 0.5i.

Figure 11 shows the real part of $E_{_}(\zeta)$ (solid) and, for comparison, the real part of the solution of the cold plasma equation [Eq. (1.4)] for the particular case K = 21. We remind the reader that in the scaled variables

$$\zeta = k_o\left(\frac{\varepsilon}{\delta}\right)^{1/2} s = \left(\frac{\omega}{v_e L}\right)^{1/2} s \quad , \tag{4.6}$$

ORNL-DWG 86-2052 FED

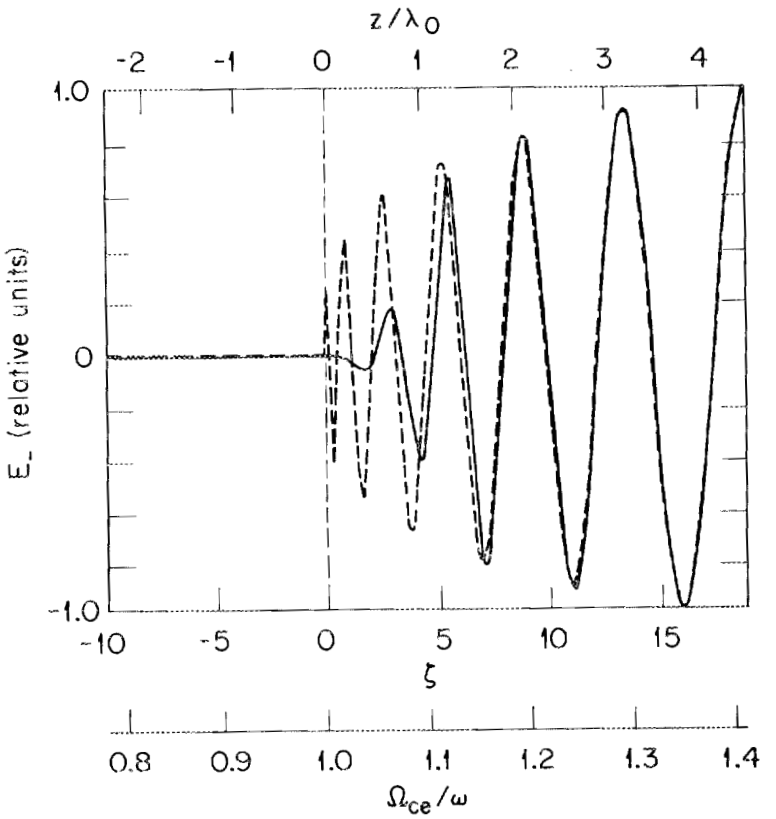

Fig. 11. Computed electric field profile E_-, real part (solid curve), imaginary part (dashed curve) versus scaled length along the field ζ when $k = 21$. Also shown are the scales in Ω_{ce}/ω and Z/λ_o for the parameter $n_e = 2 \times 10^{12}/cm^3$, $T_e = 300$ eV, $L = 12$ cm.

where s = dimensional distance along the field from the resonance layer and for the simple case $k_\perp = 0$.

$$K = \frac{\omega_{pe}^2}{\omega^2} \frac{\sqrt{\varepsilon}}{\delta^{3/2}} = \frac{\omega_{pe}^2}{\omega^2} \left(\frac{v_e}{c}\right)^{1/2} \left(k_o L\right)^{3/2} \quad . \tag{4.7}$$

A set of parameters of interest to TMX-U or EBT-S for which $K = 21$ is a reasonable value is $F = 28$ GHz, $n_e = 2 \times 10^{12}/cm^3$ $(\omega_{pe}^2/\omega^2 = 0.2)$,

T_e = 300 eV (ε = 0.034) and L = 12 cm. Figure 11 is identical to Fig. 1b of Ref. 6 except that is is plotted in our present scaled variables and also in terms of the free space wavelengths, λ_0 = 1.07 cm, for the above set of plasma parameters. The warm plasma and cold plasma results are in agreement for large ζ, $\zeta \gtrsim 8.0$. However, for $\zeta \lesssim 8$ the amplitude of the warm plasma decreases and a phase shift develops with the wavelengths of the warm plasma solution decreasing more rapidly than the cold plasma results.

Figure 12 shows the electromagnetic Poynting flux obtained from Fig. 11 and the flux obtained from warm plasma, local WKB theory by integrating k_i [Eqs. (1.8) and (1.9)]. We notice that the Poynting flux for the nonlocal calculation initially increases as might be anticipated

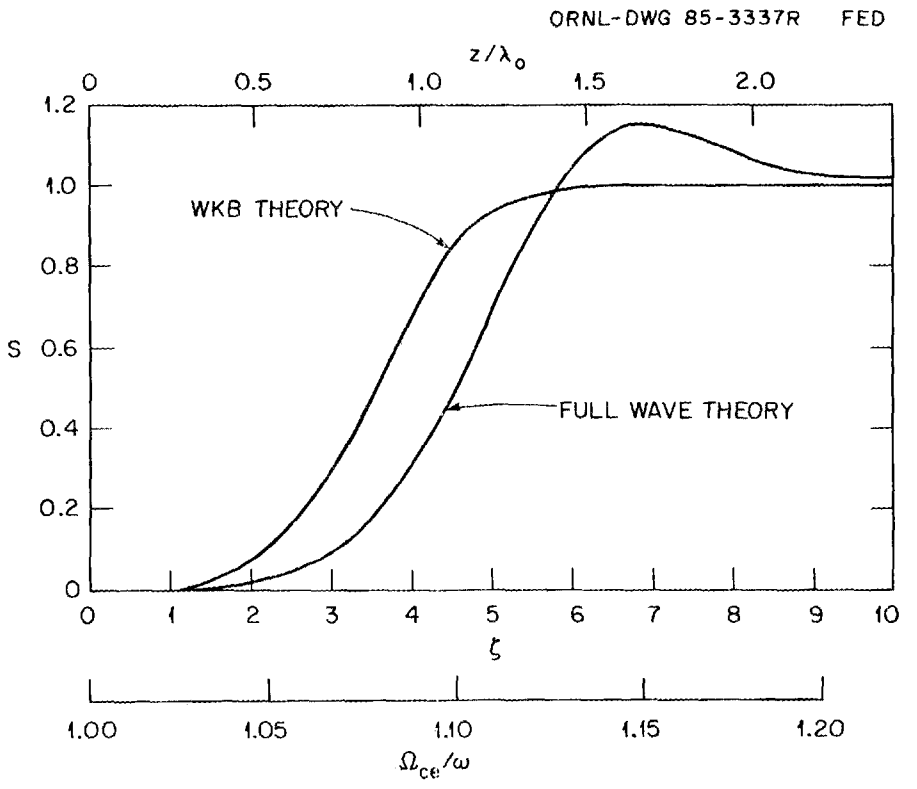

Fig. 12. Profiles of electromagnetic power flux obtained from computed full wave electric field and from local WKB calculations.

from the region of negative Re{H(x)} seen in Fig. 7 and the region of negative dissipation seen in Figs. 8 and 9. The absorption prediced by the nonlocal, full wave theory is more rapid than that prediced by WKB theory. The half power point occurs at about 30% higher magnetic field in the full wave theory.

5. DISCUSSION

In this paper we have studied the absorption of extraordinary mode waves propagating nearly along the magnetic field where the magnetic geometry has ∇B nearly parallel to $\underset{\sim}{B}$. In such geometry E_- is not shielded out by the large electron conductivity, and damping is very strong. In order to account for the strong damping and the fact that no well defined $\kappa_{\parallel}$ exists, an integrodifferential system is solved. Assuming $\delta = \lambda_o/L$ and $\varepsilon = v_{th}/c$ to be small parameters confines the resonance interaction to a thin boundary layer near the $\Omega_{ce} = \omega$ surface within which the equations can be greatly simplified. In particular, the ordering used permits the $v_{\perp}$ dependence to be separated reducing the problem to one in $v_{\parallel}$ and ζ. It should be noted that in third ordering the variation of particle $v_{\parallel}$ due to $\mu\nabla B$ forces is neglected [these would enter through order ε terms on the right side of Eq. (2.27)]. There is an additional boundary layer at $v_{\parallel} = 0$, $\rho = 0$ where upon the first two terms on the left of Eq. (2.27) vanish. This is of no consequence for the cases considered here since the wave energy is effectively gone by the point $\zeta = 0$. Calculations of quasi-linear diffusion and energy gain for single particles (such as given by Howard[8]) have shown that $\mu\nabla B$ force is important for single particles mirroring near the resonance

layer. However, our calculations show that their contribution to the plasma current does not affect the wave propagation, at least when the distribution function is Maxwellian. Of course in a strongly heated plasma with a non-Maxwellian group of energetic particles turning near resonance, this may no longer be true.

The analytic calculations presented in Sec. 3 show that the complete wave absorption seen in cold plasma theory and in warm plasma WKB theory for sufficiently dense plasmas also holds kinetically for a wide class of smooth equilibrium distribution functions. Also for low density plasmas for which there can be some transmission through the resonance, the transmission coefficients for both high and low field incidence are correctly given by the cold plasma results.

In order to obtain profiles of E_- and power absorption, it is necessary to solve the integrodifferential system numerically. Again, the calculations presented in Sec. 4 confirm the absence of a reflected wave and the complete absorption of the incident power. For the plasma paramaters used in the example presented, the nonlocally calculated power deposition profile differs quantitatively from a local WKB calculation. An interesting feature shown in Figs. 10 and 11 is the negative absorption as the wave first enters the resonance region. This is to be expected from the form of the Greens function (Fig. 8). Physically this is the result of particles with $v_{\parallel} > 0$ having the correct phase relation to return energy to the wave at large ζ, which had been absorbed from the wave in the region of strong interaction. A similar effect is seen in other situations where the wave carries a kinetic energy flux. An example is in minority ion cycloton heating in perpendicularly stratified plasmas.[9,10]

In Fig. 11 the absorption is seen to be somewhat more rapid than is predicted by the local WKB theory. Although there is probably little practical consequence of whether the power is absorbed spatially at $\Omega_{ce}/\omega = 1.07$ versus 1.13, through the Doppler shifted resonance condition, Eq. (1.10), this translates into a difference in the location in velocity space at which the wave energy is deposited. The velocity space behavior of the quasi-linear diffusion operator can be very crucial depending on the location of loss cones or the neoclassical confinement characteristics of various regions of velocity space. Work is under way to evaluate the quasi-linear operator for the self-consistent electric field obtained here. However, because of the strong damping and the rapid variation of effective $K_{\parallel}$, the usual stationary phase methods used to evaluate the quasi-linear operator in spatially varying plasmas cannot be applied.

REFERENCES

1. T. H. Stix, The Theory of Plasma Waves (McGraw Hill, New York, 1960).

2. D. B. Batchelor, Plasma Phys. 22, 41 (1980).

3. For a recent review with copious references see M. Bornatici, R. Cano, O. DeBarbieri, and F. Engelman, Nucl. Fusion 23, 1153 (1983).

4. A. V. Timofeev and G. N. Chulkov, Sov. J. Plasma Phys. 5, 712 (1980).

5. D. B. Batchelor, R. C. Goldfinger, and H. Weitzner, IEEE Trans. Plasma Sci. PS-8, 78 (1980).

6. A. Fruchtman and H. Weitzner, submitted to Phys. Fluids.

7. H. Weitzner, Phys. Fluids 26, 998 (1983).

8. J. E. Howard, Plasma Phys. 23, 597 (1981).

9. P. L. Colestock and R. J. Kashuba, Nucl. Fusion 23, 763 (1983).

10. K. Imre and H. Weitzner, Phys. Fluids 28, 3572 (1985).

ORNL/TM-10020
Dist. Category UC-20 g

INTERNAL DISTRIBUTION

1-6. D. B. Batchelor
7. C. O. Beasley
8. B. A. Carreras
9. M. D. Carter
10. E. C. Crume
11. N. O. Dominguez
12. R. A. Dory
13. C. L. Hedrick
14. S. P. Hirshman
15. J. T. Hogan
16. W. A. Houlberg
17. H. C. Howe
18. E. F. Jaeger
19. G. S. Lee
20. J. F. Lyon
21. J. A. Rome
22. K. C. Shaing
23. J. Sheffield
24. D. A. Spong
25-26. Laboratory Records Department
27. Laboratory Records, ORNL-RC
28. Document Reference Section
29. Central Research Library
30. Fusion Energy Division Library
31. Fusion Energy Division Reports Office
31. ORNL Patent Office

EXTERNAL DISTRIBUTION

32. Office of the Assistant Manager for Energy Research and Development, Department of Energy, Oak Ridge Operations Office, P. O. Box E, Oak Ridge, TN 37830
33. J. D. Callen, Department of Nuclear Engineering, University of Wisconsin, Madison, WI 53706
34. R. W. Conn, Department of Chemical, Nuclear, and Thermal Engineering, University of California, Los Angeles, CA 90024
35. S. O. Dean, Director, Fusion Energy Development, Science Applications, Inc., Gaithersburg, MD 20760
36. H. K. Forsen, Bechtel Group, Inc., Research Engineering, P. O. Box 3965, San Francisco, CA 94105
37. A. Fruchtman, Courant Institute of Mathematical Sciences, New York University, 251 Mercer Street, New York, NY 10012.
38. R. W. Gould, Department of Applied Physics, California Institute of Technology, Pasadena, CA 91125
39. D. G. McAlees, Exxon Nuclear Co., Inc., 777 106th Avenue, NE, Bellevue, WA 98009
40. K. Riedel, Courant Institute of Mathematical Sciences, New York University, New York, NY 10012.
41. H. Weitzner, Courant Institute of Mathematical Sciences, New York University, New York, NY 10012.
42. P. J. Reardon, Princeton Plasma Physics Laboratory, P. O. Box 451, Princeton, NJ 08544

43. W. M. Stacey, School of Nuclear Engineering, Georgia Institute of Technology, Atlanta, GA 30332
44. G. A. Eliseev, I. V. Kurchatov Institute of Atomic Energy, P. O. Box 3402, 123182 Moscow, U.S.S.R.
45. V. A. Glukhikh, Scientific-Research Institute of Electro-Physical Apparatus, 188631 Leningrad, U.S.S.R.
46. I. Spighel, Lebedev Physical Institute, Leninsky Prospect 53, 117924 Moscow, U.S.S.R.
47. D. D. Ryutov, Institute of Nuclear Physics, Siberian Branch of the Academy of Sciences of the U.S.S.R., Sovetskaya St. 5, 630090 Novosibirsk, U.S.S.R.
48. V. T. Tolok, Kharkov Physical-Technical Institute, Academical St. 1, 310108 Kharkov, U.S.S.R.
49. R. Varma, Physical Research Laboratory, Navangpura, Ahmedabad, India
50. Bibliothek, Max-Planck Institut fur Plasmaphysik, D-8046 Garching bei Munchen, Federal Republic of Germany
51. Bibliothek, Institut fur Plasmaphysik, KFA, Postfach 1913, D-5170 Julich, Federal Republic of Germany
52. Bibliotheque, Centre des Recherches en Physique des Plasmas, 21 Avenue des Bains, 1007 Lausanne, Switzerland
53. Bibliotheque, Service du Confinement des Plasmas, CEA, B.P. No. 6, 92 Fontenay-aux-Roses (Seine), France
54. Documentation S.I.G.N., Departement de la Physique du Plasma et de la Fusion Controlee, Centre d'Etudes Nucleaires, B.P. 85, Centre du Tri, 38041 Cedex, Grenoble, France
55. Library, Culham Laboratory, UKAEA, Abingdon, Oxon, OX14 3DB, England
56. Library, FOM-Instituut voor Plasma-Fysica, Rijnhuizen, Jutphaas, The Netherlands
57. Library, Institute of Physics, Academia Sinica, Beijing, Peoples Republic of China
58. Library, Institute of Plasma Physics, Nagoya University, Nagoya, Japan
59. Library, International Centre for Theoretical Physics, Trieste, Italy
60. Library, Laboratorio Gas Ionizatti, Frascati, Italy
61. Library, Plasma Physics Laboratory, Kyoto University, Gokasho Uji, Kyoto, Japan
62. Plasma Research Laboratory, Australian National University, P.O. Box 4, Canberra, A.C.T. 2000, Australia
63. Thermonuclear Library, Japan Atomic Energy Research Institute, Tokai, Naka, Ibaraki, Japan
64. J. F. Clarke, Associate Director for Fusion Energy, Office of Fusion Energy, Office of Energy Research, U.S. Department of Energy, Mail Stop G-256, Washington, DC 20545
65. D. B. Nelson, Acting Director, Division of Applied Plasma Physics, Office of Fusion Energy, Office of Energy Research, U.S. Department of Energy, Mail Stop G-256, Washington, DC 20545
66. W. Sadowski, Fusion Theory and Computer Services Branch, Office of Fusion Energy, Office of Energy Research, U.S. Department of Energy, Mail Stop G-256, Washington, DC 20545

67. N. A. Davies, Tokamak Systems Branch, Office of Fusion Energy, Office of Energy Research, U.S. Department of Energy, Mail Stop G-256, Washington, DC 20545
68. E. Oktay, Tokamak Systems Branch, Office of Fusion Energy, Office of Energy Research, U.S. Department of Energy, Mail Stop G-256, Washington, DC 20545
69. M. N. Rosenbluth, University of Texas, Institute for Fusion Studies, RLM 11.218, Austin, TX 78712
70. Theory Department Read File, c/o D. W. Ross, University of Texas, Institute for Fusion Studies, Austin, TX 78712
71. Theory Department Read File, c/o R. C. Davidson, Director, Plasma Fusion Center, NW 16-202, Massachusetts Institute of Technology, Cambridge, MA 02139
72. Theory Department Read File, c/o F. W. Perkins, Princeton Plasma Physics Laboratory, P.O. Box 451, Princeton, NJ 08544
73. Theory Department Read File, c/o L. Kovrizhnikh, Lebedev Institute of Physics, Academy of Sciences, 53 Leninsky Prospect, 117924 Moscow, U.S.S.R.
74. Theory Department Read File, c/o B. B. Kadomtsev, I. V. Kurchatov Institute of Atomic Energy, P.O. Box 3402, 123182 Moscow, U.S.S.R.
75. Theory Department Read File, c/o T. Kamimura, Institute of Plasma Physics, Nagoya University, Nagoya, Japan
76. Theory Department Read File, c/o C. Mercier, Euratom-CEA, Service des Recherches sur la Fusion Controlee, Fontenay-aux-Roses (Seine), France
77. Theory Department Read File, c/o T. E. Stringer, JET Joint Undertaking, Culham Laboratory, Abingdon, Oxon OX14 3DB, England
78. Theory Department Read File, c/o K. Roberts, Culham Laboratory, Abingdon, Oxon OX14 3DB, England
79. Theory Department Read File, c/o D. Biskamp, Max Planck Institut fur Plasmaphysik, D-8046 Garching bei Munchen, Federal Republic of Germany
80. Theory Department Read File, c/o T. Takeda, Japan Atomic Energy Research Institute, Tokai, Naka, Ibaraki, Japan
81. Theory Department Read File, c/o C. S. Liu, GA Technologies, Inc., P.O. Box 81608, San Diego, CA 92138
82. Theory Department Read File, c/o L. D. Pearlstein, Lawrence Livermore National Laboratory, P.O. Box 808, Livermore, CA 94550
83. Theory Department Read File, c/o R. Gerwin, CTR Division, Los Alamos National Laboratory, P.O. Box 1663, Los Alamos, NM 87545
84. T. Amano, Institute of Plasma Physics, Nagoya University, Nagoya, Japan
85. C. D. Boley, Fusion Power Program, Building 207C, Argonne National Laboratory, Argonne, IL 60439
86. Yu. N. Dnestrovskii, I. V. Kurchatov Institute of Atomic Energy, P.O. Box 3402, 123182 Moscow, U.S.S.R.
87. J. Gaffey, IPST, University of Maryland, College Park, MD 20742
88. R. J. Hawryluk, Princeton Plasma Physics Laboratory, P.O. Box 451, Princeton, NJ 08544
89. W. W. Pfeiffer, GA Technologies, Inc., P.O. Box 81608, San Diego, CA 92138

90. D. E. Post, Princeton Plasma Physics Laboratory, P.O. Box 451, Princeton, NJ 08544
91. A. Ware, Physics Department, University of Texas, Austin, TX 78712
92. J. Wiley, University of Texas, Institute for Fusion Studies, Austin, TX 78712
93. S. K. Wong, GA Technologies, Inc., P.O. Box 81608, San Diego, CA 92138
94. S. Yoshikawa, Princeton Plasma Physics Laboratory, P.O. Box 451, Princeton, NJ 08544

95-248. Given distribution as shown in TID-4500, Magnetic Fusion Energy (Distribution Category UC-20g, Theoretical Plasma Physics)